

Research article

Spatial Analysis of Flood-Prone Areas in Padang Terap, Kedah: Integrating Spatial Autocorrelation and Optimized Hotspot Analysis

Azizul Ahmad¹, Mohd Zulhafiz Said^{2*}, Salfarina Abdul Gapor³, Lindah Roziani Jamru⁴, Norita Jubit⁵, Sumayyah Aimi Mohd Najib⁶, Tarmiji Masron¹, Nur Afiqah Ariffin⁷, and Yaniza Shaira Zakaria⁸

¹ Centre for Spatially Integrated Digital Humanities (CSIDH), Faculty of Social Sciences & Humanities (FSSH), Universiti Malaysia Sarawak (UNIMAS), Datuk Mohammad Musa Road, 94300 Kota Samarahan, Sarawak, Malaysia; ² Faculty of Human Ecology, Universiti Putra Malaysia, 43400 UPM Serdang, Selangor Malaysia; ³ School of Business and Social Sciences, Albukhary International University, Jalan Tun Abdul Razak, 05200, Alor Setar, Kedah, Malaysia; ⁴ Geographic Section, Faculty Social Sciences & Humanities, Universiti Malaysia Sabah (UMS), 88400 Kota Kinabalu, Sabah, Malaysia; ⁵ Borneo Institute for Indigenous Studies (BorIIS), Universiti Malaysia Sabah (UMS), 88400 Kota Kinabalu, Sabah, Malaysia; ⁶ Faculty of Human Sciences, Universiti Pendidikan Sultan Idris (UPSI), 35900 Tanjung Malim, Perak, Malaysia; ⁷ HS Innovators Sdn Bhd, No 5U-1A-04 Tingkat 1, Blok 5, Pusat Daerah Seksyen 6, Jalan Cenderawasih 6/7, Seksyen 6, 40000 Shah Alam, Selangor, Malaysia; ⁸ Institute of Oceanography and Environment (INOS), Universiti Malaysia Terengganu, 21030 Kuala Nerus, Terengganu, Malaysia.

^{*}Correspondence: mohdzulhafiz@upm.edu.my

Citation:

Ahmad, A., Said, M. Z., Gapor, S. A., Jamru, L. R., Jubit, N., Najib, S. A. M., Masron, T., Ariffin, N. A., & Zakaria, Y. S. (2026). Spatial Analysis of Flood-Prone Areas in Padang Terap, Kedah: Integrating Spatial Autocorrelation and Optimized Hotspot Analysis. *Forum Geografi*. 40(1), 19-43.

Article history:

Received: 6 May 2025
Revised: 30 November 2025
Accepted: 6 January 2026
Published: 22 January 2026

Abstract

Flooding increasingly threatens socio-economic resilience in Malaysia, particularly in vulnerable districts such as Padang Terap, Kedah. Using a GIS-based framework integrating Spatial Autocorrelation (Moran's I) and Optimized Hotspot Analysis (Getis-Ord Gi*), this study quantifies spatial clustering of flood-prone areas across four inundation levels (0.3 m–3.7 m). Results reveal intensifying positive spatial autocorrelation with rising flood depths, reflecting hydrological connectivity and topographic controls. Hotspots are consistently concentrated in Belimbing Kanan, Belimbing Kiri, and Padang Temak, emphasizing severe spatial heterogeneity in flood risk distribution. These findings demonstrate that flood hazards are not randomly dispersed but spatially structured, necessitating geographically targeted risk mitigation strategies. Incorporating hotspot insights into planning can optimize resource allocation, strengthen adaptive capacity, and inform flood-resilient urban development. This research advocates for integrating fine-scale spatial analyses into national disaster frameworks to enhance Malaysia's climate resilience agenda. Future work should embed socio-economic vulnerability metrics and spatiotemporal models to refine flood risk governance and promote equitable, anticipatory disaster management.

Keywords: flood prone area; optimized hotspot analysis; padang terap; spatial analysis; spatial autocorrelation.

1. Introduction

Malaysia has long struggled with recurring flood disasters, particularly from 2000 to 2025 (Karim *et al.*, 2016; Romali & Yusop, 2021; Yusoff *et al.*, 2017). These disasters are primarily driven by climatological factors such as rainfall distribution, evaporation, wind movement, temperature variations, and the Earth's surface conditions (Balek, 1983; Gasim *et al.*, 2010; Utama *et al.*, 2019). An estimated 29,800 square kilometres of land in Malaysia are considered flood-prone (Buslima *et al.*, 2018), making floods one of the most significant natural threats to national development. The impacts of flooding are far-reaching, with severe consequences for people, infrastructure, and the economy. For instance, nationwide floods in 2006 and 2007 resulted in losses of RM1.1 billion and RM776 million, respectively (Berita Harian, 2007). In December 2024, Malaysia again faced devastating floods, especially in Kelantan and Terengganu. According to the National Disaster Management Agency (NADMA), approximately 137,410 individuals were affected, with 40,922 displaced families sheltered in 633 temporary relief centres. Tragically, five fatalities were reported (reliefweb, 2024). The Deputy Prime Minister described these floods as the worst since 2014, highlighting widespread damage to homes, transportation infrastructure, and public utilities, particularly in the East Coast states (reliefweb, 2025). Although the total financial losses are still being calculated, Prime Minister Anwar Ibrahim estimated that repair costs could reach RM1 billion (US\$224 million) (apnews, 2024). These figures may continue to rise as the monsoon season persists until March, bringing more rainfall and compounding the damage (Nair & Aravind, 2020). Historically, the Malaysian government has invested heavily in flood mitigation. In 2001 and 2006, RM1.79 billion and RM5.81 billion were spent, respectively, on flood control systems. Additionally, RM100 million was allocated to the Department of Irrigation and Drainage (JPS) in 2009 for river maintenance across the country (Kathirguman, 2021; Shahrulnizam *et al.*, 2020).

One of the most affected states is Kedah, which has repeatedly suffered from flood events, resulting in major financial and social disruptions. Between 2000 and 2010, flood-related damages in Kedah increased, with the worst losses recorded in 2010, amounting to RM17.82 million. That



Copyright: © 2026 by the authors. Submitted for possible open access publication under the terms and conditions of the Creative Commons Attribution (CC BY) license (<https://creativecommons.org/licenses/by/4.0/>).

year, over 50,000 people were evacuated, and critical infrastructure, including the North-South Expressway, railway lines, and Sultan Abdul Halim Airport, was forced to close. The floods also devastated rice production in Kedah and Perlis, with over 45,000 hectares of paddy fields damaged. In response, the government pledged RM26 million in aid to farmers (Bernama, [2010](#)). The Padang Terap district in Kedah is a particularly notable case. With a history of flood events dating back to 1937, Padang Terap has consistently experienced worsening flood intensity and frequency (Said *et al.*, [2024](#)). Between 2000 and 2010, the district recorded cumulative losses of RM16.62 million, with RM5.7 million in damages occurring in 2010 alone (Said *et al.*, [2024](#)). In that year, the government provided RM500 in compassionate assistance to each affected household, amounting to RM45.08 million nationwide RM20.41 million of which was designated for Kedah residents (reliefweb, [2010](#)). These trends illustrate the escalating financial burden and rising vulnerability of flood-prone areas like Padang Terap, underscoring the urgent need for strategic flood risk management and resilience-building initiatives. One of the major limitations in current flood management efforts is the reactive, ad hoc nature of response strategies. Despite substantial financial allocations, many communities remain highly vulnerable, largely due to weak adaptation systems and a lack of preparedness. Effective flood risk management must go beyond disaster response; it must focus on empowering communities to transition from being “unprepared” to “prepared,” and from “vulnerable” to “resilient” (reliefweb, [2010](#); Rosmadi *et al.*, [2023](#)).

In this context, hotspot analysis becomes critically important. It involves identifying and mapping high-risk areas based on historical flood data, environmental conditions, and socio-economic vulnerabilities. This targeted approach enables decision-makers to prioritise interventions in areas most susceptible to flooding. Hotspot analysis enhances the efficiency of resource allocation, ensuring that flood mitigation efforts, such as early warning systems, drainage upgrades, and community education programs, are implemented where they are most urgently needed. It also offers deeper insights into the underlying causes of vulnerability, enabling context-specific adaptation strategies. For instance, understanding why Padang Terap continues to suffer significant losses despite decades of investment can inform better solutions that address the district's unique geographical and social realities. On a national scale, hotspot analysis can guide infrastructure planning, policy formulation, and climate resilience strategies, reducing the risk of repeating past mistakes and improving the nation's preparedness for future disasters. Adaptation, in this regard, refers to proactive recovery measures that help communities adjust to the impacts of flood hazards, thereby reducing damage and losses (Tanoue *et al.*, [2021](#)). As Malaysia strives toward developed nation status, it must strengthen its adaptive capacity to confront the escalating challenges of climate change and global warming, which are intensifying the frequency and severity of flood events. Complicating matters further is the lack of detailed knowledge about flood-prone populations and their specific vulnerabilities (Singer, [2018](#)). This gap highlights the need for robust data collection and community-level flood risk assessments. Residents, local authorities, and government agencies must be equipped with the knowledge and tools to better prepare for floods, mitigate risks, and adopt effective adaptation strategies. Otherwise, if current trends persist, more areas and populations will become vulnerable, and the associated losses, both human and financial, will continue to escalate (Krichene *et al.*, [2023](#)). Identifying and analysing flood-prone communities is essential for understanding the characteristics that contribute to their vulnerability and for assessing whether current adaptation measures are effective. Ultimately, these analyses can drive more informed and strategic improvements in flood risk governance, reducing exposure and enhancing resilience across the country (Rubio *et al.*, [2020](#)).

2. Literature Review

Vulnerability, in the context of flood events, is a complex and multifaceted concept that extends beyond mere exposure to risk. It encompasses the interplay of physical, social, economic, and environmental factors that either amplify or reduce the potential for harm. According to the IPCC, vulnerability is defined as a function of exposure, sensitivity, and adaptive capacity (An *et al.*, [2021](#)). It is not merely the susceptibility to damage, but a dynamic process shaped by adaptability and resilience, representing the capacity of a system to "bounce back" from adverse impacts (Salignac *et al.*, [2022](#)). Vulnerability emerges from the convergence of social and physical conditions that make elements of urban or ecological systems susceptible to harm (Müller *et al.*, [2011](#)). A key physical component is exposure to the hazard, which highlights the risk faced by people and infrastructure in the absence of adequate protective measures. This lack of protection often stems from socioeconomic factors such as income disparities, occupational hazards, limited access to information technology, and restricted financial resources (Eze *et al.*, [2018](#)). Beyond exposure, the concept also integrates sensitivity to flood impacts and the adaptive capacity to recover from them (Rezende *et al.*, [2020](#)). Vulnerability is not static, it varies across time and space due to differences in environmental conditions, societal norms, and human activities (Nasiri *et al.*, [2016](#)).

Its significance and the degree of exposure play a role in determining the level of adaptive capacity needed (Abante, 2021). Therefore, reducing vulnerability is key to successful adaptation strategies (Kreibich *et al.*, 2017), and understanding its drivers is crucial for designing targeted interventions (Kashyap & Mahanta, 2021).

The clustering of flood incidences in Padang Terap can be partly attributed to long-term persistence (LTP) in hydrological variables, a phenomenon first noted by Hurst and often termed the Hurst phenomenon or Hurst–Kolmogorov (HK) dynamics (Hurst, 1951). In long-memory time series, runs of extreme values tend to cluster, producing extended wet or dry periods. For example, O’Connell *et al.* (2022) emphasizes that large-scale precipitation and runoff records often exhibit high Hurst coefficients, meaning multiyear sequences of above- or below-average conditions. In practice, this means persistent rainfall or runoff anomalies can drive successive flood events across adjacent basins. Recent analyses confirm that aggregated precipitation over regional scales shows pronounced long-term dependence, which in turn induces LTP in river flows (O’Connell *et al.*, 2022). Papoulakos *et al.* (2025) demonstrate this effect: they found clear deviations from independent flood-event assumptions, with streamflow extremes showing significant clustering and a “persistent behavior” consistent with HK dynamics. In other words, floods do not occur as isolated events but tend to group in space–time under slowly varying climate drivers. In Padang Terap, the strong spatial autocorrelation of flood-prone zones may thus reflect these underlying hydrometeorological memories: when broad-scale weather patterns produce sustained heavy rainfall or runoff, neighboring areas are likely to flood together. In summary, the Hurst phenomenon implies that flood risk in one year or location is correlated with risk in following years or adjacent areas, helping explain the observed hotspot clustering in the GIS analysis (O’Connell *et al.*, 2022; Papoulakos *et al.*, 2025).

Adaptation in flood risk management refers to the process of adjusting to actual or anticipated climate change effects to moderate harm or take advantage of opportunities. These strategies must be deeply rooted in the local context, reflecting the specific vulnerabilities and capacities of the affected communities (Bukvic *et al.*, 2020). Adaptation can be reactive or anticipatory, spontaneous or planned, and may involve transformations in infrastructure, behaviour, policies, and social norms (Hussain *et al.*, 2021). Given the place-specific nature of flood risks, adaptation measures must be tailored to the local frequency and intensity of floods, demographic factors, and resource availability. Examples of adaptation include large-scale infrastructure such as seawalls and dams, as well as smaller initiatives like flood-resistant construction and early warning systems. In developing countries, outdated urban infrastructure poses a major challenge in coping with increased precipitation due to climate change (Kim *et al.*, 2016). Flood-proofing is an effective adaptive strategy, reducing building vulnerability and extending infrastructure lifespan (Madhuri *et al.*, 2021). Geographic Information Systems (GIS) play a pivotal role in flood vulnerability assessment and adaptation planning. One of its key tools, hotspot analysis, helps identify spatial clusters where flood risk or impact is significantly elevated (Lessy *et al.*, 2018). By leveraging spatial statistics, GIS reveals patterns in flood occurrences, vulnerabilities, and potential impacts, thus informing targeted interventions and efficient resource allocation. It integrates diverse data sources, such as topographical information, hydrological models, land use, socioeconomic indicators, and historical flood records, into a comprehensive geospatial framework for analysis (Baky *et al.*, 2020; Nugraha, 2018).

2.1. Urban Expansion and Floodplain Encroachment

A reverse causality also operates: growing urban settlements increasingly drive flood risk by encroaching on floodplains. Rapid development replaces natural buffer zones with impermeable surfaces, boosting runoff and exposure. In Malaysia, scholars note that uncontrolled urban growth “has destroyed pervious surfaces” and significantly heightened flash-flood vulnerability (Kumaresen *et al.*, 2025). N. Wang *et al.* (2023) quantified a global pattern: in more than half of examined countries people are moving away from rivers to reduce casualties, yet where flood-protection infrastructure exists, communities stay closer and “human–flood distance” even decreases. In other words, while some retreat occurs, new construction often proceeds right into formerly risky areas under the illusion of safety. Case studies illustrate this trend: as Greater Kuala Lumpur expands, natural floodplains are “replaced with concrete structures,” drastically reducing water absorption and amplifying runoff during storms (Abid *et al.*, 2024). The 2021–2022 Malaysian floods underscored this dynamic by devastating areas that had been heavily developed for housing and agriculture. Thus, in Padang Terap the spatial flood vulnerability identified by hotspot analysis is likely reinforced by settlement patterns: villages and farms have sprawled onto low-lying terrain and riparian zones. This matches the global finding of N. Wang *et al.* (2023) that urban sprawl in floodplains intensifies flood exposure. In short, increased urbanization in

Malaysia not only suffers from floods but actively exacerbates them by encroaching on natural drainage corridors (Abid *et al.*, 2024).

2.2. Comparative Flood Vulnerability: Padang Terap, Kelantan, and Jakarta

Padang Terap's flooding can be contrasted with other regional hotspots to highlight distinctive pressures. In Kelantan (Peninsular Malaysia's northeast coast), flood risk is driven by seasonal Northeast Monsoon rainfall that swells the Kelantan River basin. In fact, Malaysia "experiences seasonal floods, particularly during the Northeast Monsoon" that heavily impact Kelantan (among other states) (Abid *et al.*, 2024). Like Padang Terap, Kelantan's threat is mostly hydrometeorological: it stems from intense rainfall over floodplains. However, Kelantan is even more exposed due to its location on Malaysia's flood-prone east coast, and studies have documented severe inundations and erosion in its river network. In contrast, Jakarta's floods illustrate a heavily urbanized context. Continuing urbanization in Jakarta has dramatically increased flood vulnerability especially in river-adjacent slum areas (Nasution *et al.*, 2022). Nasution *et al.* (2022) report that as floods become routine in Jakarta, unabated urban sprawl (often on reclaimed or subsiding land) leads to routine inundation, with more severe floods occurring when large rivers overflow. The March 2025 Jakarta disaster (over 100,000 people displaced by 1–3 m of water) exemplifies how dense development and aging infrastructure amplify climate threats. By comparison, Padang Terap's setting is rural: its flood hotspots arise from upland rainfall and river dynamics more akin to Kelantan's monsoonal pattern, rather than Jakarta's fast-flash, drainage-limited regime. This suggests that while all three regions face flood exposure and development pressures, the underlying mechanisms differ. Kelantan and Padang Terap share pronounced hydroclimatic drivers and contiguous floodplain inundation, whereas Jakarta's hazard is worsened by impervious surfaces, land subsidence, and inadequate urban drainage (Abid *et al.*, 2024; Nasution *et al.*, 2022). Recognizing these differences is critical for resilience: Padang Terap (and Kelantan) may benefit most from catchment-level land management and green infrastructure, whereas Jakarta-like contexts require aggressive urban planning, drainage upgrades, and subsidence control.

3. Methodology and Study Area

Spatial data often exhibit patterns that provide insights into the underlying processes shaping geographical phenomena. Two critical concepts used in analyzing such patterns are Spatial Autocorrelation and Optimized Hotspot Analysis. These tools are particularly effective for analyzing the spatial patterns of events such as crime incidents, disease outbreaks, or environmental hazards, offering a concise representation of complex spatial data (Jamru *et al.*, 2024; Masron, Ahmad, Abdillah, Junaini, *et al.*, 2025; Masron *et al.*, 2024; Redzuan *et al.*, 2025; Zakaria, Ariffin, *et al.*, 2025).

3.1. Study Area

In 2010, the Padang Terap District in Kedah was significantly affected by flooding, with 11 sub-districts impacted (Table 1). Although specific evacuation figures for Padang Terap were not detailed in available reports, statewide data indicated that more than 28,000 people had been evacuated in Kedah as of November 4, 2010, with conditions in Padang Terap reportedly beginning to improve at that time (The Star, 2010). Despite the lack of detailed statistics for that year, Padang Terap has continued to face severe flooding in subsequent years. For example, in November 2024, a total of 1,298 individuals from 386 families were reported to be affected by floods in the district (Hilmy, 2024). According to data from the Department of Social Welfare (JKM), a total of 1,427 families were registered as victims during the 2010 flood. For the purposes of this study, a sample size of 680 individuals representing 47.7% of the affected population was selected. It is important to note that not all those registered with JKM were considered respondents, as some were stranded due to the flood but did not experience direct flooding of their homes. Consequently, only those whose residences were inundated were included in the study sample.

According to the research findings, recorded floodwater levels were observed at 0.3 meters, 2.0 meters, 2.5 meters, and 3.7 meters. These measurements indicate the vertical height of floodwaters in relation to the highest structural point of the affected houses, typically the floor level or platform of the living area. A flood level of 0.3 meters suggests minor inundation, likely affecting only ground-level areas such as yards or steps. However, levels reaching 2.0 meters or more signify severe flooding, with water submerging significant portions of the house, including interior spaces, furniture, and electrical systems. The highest recorded level of 3.7 meters implies a catastrophic flood event, likely overwhelming entire homes and posing serious threats to safety, property, and livelihood. These data points underscore the varying degrees of flood impact and highlight the vulnerability of residential structures depending on their elevation and proximity to flood-prone areas (Said, 2017).

Table 1. Sub-District Study Area.

Sub-District	Number of Respondents
Batang Tunggang Kanan	7
Batang Tunggang Kiri	19
Belimbang Kanan	164
Belimbang Kiri	187
Kurung Hitam	67
Padang Temak	83
Padang Terap Kanan	83
Padang Terap Kiri	30
Pedu	12
Tekai Kiri	14
Tekai Kanan	14
Total	680

3.2. Study Area

Padang Terap, located in the northern state of Kedah, Malaysia, represents a quintessential example of a district characterized by a mosaic of agricultural landscapes interspersed with rural settlements (Figure 1). The district's socio-economic fabric is largely shaped by its agrarian economy, yet it remains highly vulnerable to seasonal flooding events, particularly during the Northeast Monsoon period, which typically spans from November to March (Said, [2017](#)). The principal drivers of flooding in Padang Terap are multifaceted, involving both natural and anthropogenic factors. High-intensity rainfall associated with the monsoonal system exerts substantial hydrological pressure on local river systems, most notably the Sungai Padang Terap, which frequently overflows its banks, inundating adjacent settlements and farmlands. Moreover, the district's hydrological vulnerability is exacerbated by the inadequacy of drainage infrastructure, which is often insufficient to cope with the volume and velocity of stormwater runoff during peak rainfall events. Topographic elements also play a critical role; large expanses of low-lying terrain within Padang Terap act as natural basins that accumulate water, prolonging the duration of flood events and heightening the risks to both human livelihoods and agricultural productivity. These compounded factors not only amplify the frequency and severity of flood occurrences but also reveal significant challenges in local flood management strategies, highlighting a pressing need for integrated, adaptive, and resilient planning approaches that incorporate hydrological modeling, sustainable land use practices, and community-based disaster risk reduction initiatives (Said *et al.*, [2024](#)).

Padang Terap (Figure 1), a district in Kedah, Malaysia, spans approximately 1,338.70 square kilometers and is the second-largest district in the state after Sik. Bordered by Thailand to the north (at Durian Burung), Bekort to the east, and Pokok Sena to the south, the district is a vital hub for administration and agriculture. Kuala Nerang, the main town, functions as a key transit point for travelers from Alor Setar and Pokok Sena heading toward Durian Burung. It also hosts the bustling Pekan Nat market, where locals gather every Saturday and Tuesday to purchase daily necessities (Pejabat Daerah dan Tanah Padang Terap, [2016](#)). Padang Terap is characterized by a mix of flatlands and hilly terrain, including limestone outcrops. The flatter areas are predominantly used for agriculture, with rice, sugarcane, oil palm, and vegetables being the main crops. Most rural settlements are located within these zones. Despite the development of infrastructure such as paved roads, clean water access, telecommunications, and internet coverage across its 12 mukims (sub-districts) flooding remains a major environmental challenge (jps@komuniti, [2011](#)).

The district is particularly prone to seasonal flooding, especially during the Northeast Monsoon (November to March). Prolonged and heavy rainfall during this period often leads to water accumulation in low-lying and poorly drained areas. The topography of Padang Terap, marked by extensive floodplains and inadequate drainage infrastructure, further exacerbates the situation. Many drainage systems, both natural and artificial, are insufficient to cope with the volume of water, resulting in widespread and prolonged inundation (Mohamad Rosni, [2024](#)). A key contributor to flooding is the overflow of Sungai Padang Terap, the district's main river. Intense rainfall causes the river to swell beyond capacity, flooding adjacent settlements and farmlands. The risk increases significantly when upstream catchment areas also receive heavy rain, sending large volumes of water downstream. Historical flood events have shown that the river's overflow can affect areas beyond Padang Terap, including Kubang Pasu and Kota Setar (Malay Mail, [2024](#)). Agriculture, particularly paddy farming, is severely impacted by these recurring floods. Farmers rely heavily on river and rainwater irrigation, making them especially vulnerable to environmental disruptions. Floods have led to considerable crop damage, with the worst recorded loss occurring

in 2005 when approximately 13,870.31 hectares of paddy fields were destroyed. In contrast, the smallest impact was noted in 2010, affecting just 604.4 hectares (Fizri *et al.*, 2014). The persistent threat of flooding underscores the urgent need for comprehensive flood mitigation strategies. These should include enhanced drainage systems, river embankments, and sustainable land use planning to bolster community resilience. Without such measures, both the livelihoods of residents and the sustainability of local agriculture will remain at significant risk (Said *et al.*, 2024).

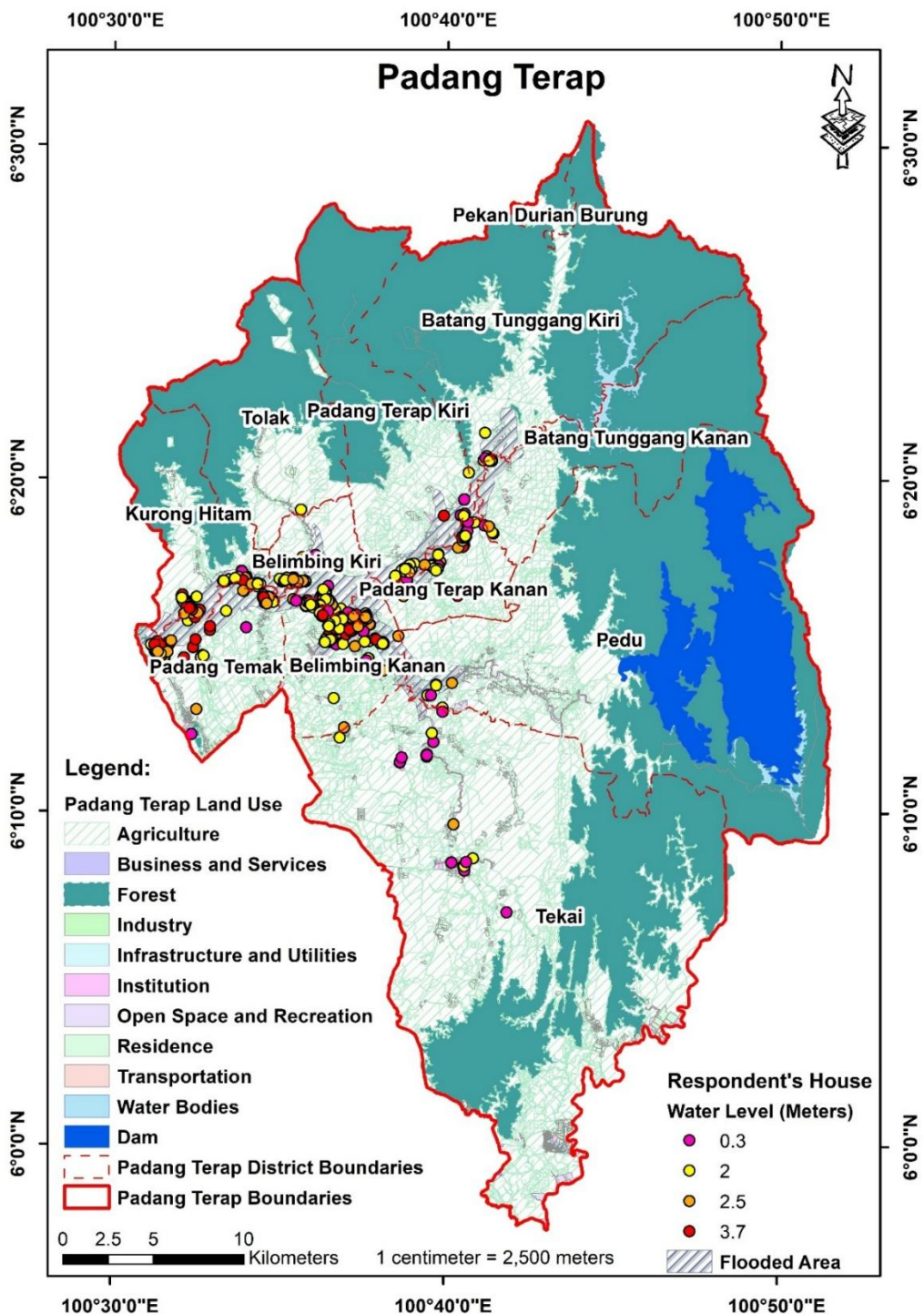


Figure 1. Study Area in Padang Terap.

3.3. Spatial Autocorrelation (SAC) (Global Moran's I): Measuring Spatial Relationships

Spatial autocorrelation quantifies the degree to which the presence, value, or distribution of a spatial phenomenon is similar across nearby geographic locations. Essentially, it evaluates whether spatial patterns are random, clustered, or evenly dispersed. When values at nearby locations

are similar, spatial autocorrelation is positive; when dissimilar values are close to each other, it is negative. If no discernible pattern exists, the data exhibit zero spatial autocorrelation. Key statistical measures, such as Moran's I and Geary's C, are commonly used to evaluate spatial autocorrelation. Moran's I provides a global assessment, measuring the overall pattern across the entire study area (Chen, 2023). A positive Moran's I value indicates clustering of similar values, while a negative value suggests dispersion. Conversely, Geary's C focuses on local differences, making it more sensitive to spatial variations at smaller scales. Spatial autocorrelation is crucial for understanding spatial dependencies and processes. For example, in flood-prone areas like Padang Terap, spatial autocorrelation can reveal whether flood incidents are clustered in specific regions or evenly distributed. A high degree of positive autocorrelation might indicate the influence of shared environmental factors, such as topography or land use, driving flood occurrences in certain areas.

Global Moran's I is a classical measure of global spatial autocorrelation that tests whether high or low values of a variable cluster in space. It is Equation 1:

$$I = \frac{n \sum_{i=1}^n \sum_{j=1}^n w_{ij} (x_i - \bar{x})(x_j - \bar{x})}{S_0 \sum_{i=1}^n (x_i - \bar{x})^2} \quad (1)$$

where x_i is the attribute value at feature i , \bar{x} is the mean of all values, w_{ij} is the spatial weight between features i and j (reflecting their spatial proximity), n is the number of features, and $S_0 = \sum_{i=1}^n \sum_{j=1}^n w_{ij}$ is the sum of all weights (Ariffin, 2022; Baykal, 2025). The choice of w_{ij} embodies the "conceptualization of spatial relationships" (e.g. fixed distance bands or contiguity) and strongly influences the results (ESRI, 2022b; C. Zhou *et al.*, 2025). Under the null hypothesis of spatial randomness, the expected value of Moran's I is $E[I] = -1/(n - 1)$, and its variance can be derived from higher-order moments of the distribution (C. Zhou *et al.*, 2025). A standardized z-score is then computed as Equation 2:

$$z_I = \frac{I - E[I]}{\sqrt{Var(I)}}, \quad (2)$$

using either analytical moments or a permutation (randomization) approach to approximate the null distribution (Baykal, 2025; ESRI, 2022b). When the sample size is large, z_I is approximately normally distributed, allowing a significance test (ESRI, 2022b).

Interpretation of Moran's I follows the rule that values near +1 indicate strong clustering of similar values (positive autocorrelation), values near -1 indicate dispersion of dissimilar values (negative autocorrelation), and values near 0 imply spatial randomness (no autocorrelation) (Baykal, 2025; ESRI, 2022b). Thus a significantly positive I (large positive z_I , small p-value) shows that high (or low) values are more spatially clustered than expected by chance, whereas a significantly negative I shows a checkerboard or alternating pattern. In practice, p-values are obtained by comparing the observed I (or its z -score) to the permutation distribution; for example, Baykal (2025) reports that in forest-fire data Moran's I values significantly above zero (with $p < 0.05$) indicate meaningful clustering. ArcGIS's Spatial Autocorrelation tool automatically computes I , $E[I]$, $Var(I)$, z -score and p-value for the input data (ESRI, 2022b). A positive Moran's I is declared significant if the z -score exceeds the critical threshold (e.g. $z > 1.96$ for 5% level) (ESRI, 2022b). Previous Malaysian studies similarly applied Moran's I to crime incidence and disease data, interpreting a significant positive index as indicating hotspots (Ariffin, 2022; Mohamad Rasidi *et al.*, 2013; Muhammad Ludin *et al.*, 2013). In summary, Global Moran's I provides a rigorous test for global clustering in the flood-risk indicator, combining spatial weights with attribute variance.

3.4. Optimized Hotspot Analysis (Getis-Ord Gi*)

Hotspot analysis, particularly using the Getis-Ord Gi* statistic, is a powerful method for identifying statistically significant clusters of high or low values within spatial data. Unlike global measures, which provide an overarching view of spatial patterns, the Getis-Ord Gi* statistic focuses on identifying local clusters or "hotspots." A hotspot is a cluster of high values surrounded by other high values, while a cold spot is a cluster of low values surrounded by other low values. The Gi* statistic evaluates whether the local sum of a variable (e.g., flood frequency) is significantly different from the expected sum in a random distribution (ArcGIS Pro 3.3, 2024a). The result is expressed as a z-score, where higher positive values indicate hotspots, and higher negative values indicate cold spots. For instance, in a study of flood incidents in Padang Terap, hotspot analysis could highlight villages or regions with frequent and intense flooding. By applying the Getis-Ord Gi* statistic to spatial data, researchers can identify statistically significant hotspots and prioritize these areas for targeted mitigation efforts. This method not only pinpoints high-risk

zones but also provides a scientific basis for resource allocation and disaster preparedness (ArcGIS Pro 3.3, 2024b).

To identify local clusters of high or low values (hotspots and coldspots), we use the Getis-Ord Gi* statistic within ArcGIS's Optimized Hot Spot Analysis. The Gi* statistic for each feature *i* compares the local sum of values in its neighborhood to the expected sum under spatial randomness (Getis & Ord, 1992). Following the formulation of Baykal (2025), the statistic is given by Equation 3:

$$G_i^* = \frac{\sum_{j=1}^n w_{ij}x_j - \bar{X} \sum_{j=1}^n w_{ij}}{S \sqrt{\left[n \sum_{j=1}^n w_{ij}^2 - (\sum_{j=1}^n w_{ij})^2 \right] / (n-1)}} \quad (3)$$

where x_j are the attribute values of features within the neighborhood of feature *i*, $\bar{X} = (1/n) \sum_{j=1}^n x_j$ is the global mean of the attribute, and $S = \sqrt{(\sum_j x_j^2/n - \bar{X}^2)} / n$ is the global standard deviation (Baykal, 2025). Here w_{ij} again denotes the spatial weight between feature *i* and neighbor *j*; in practice we use a fixed distance band or optimized distance so that each feature has a relevant set of neighbors. The Gi* statistic is essentially a normalized sum and is itself a z-score (i.e. unit normal under the null) (Baykal, 2025; ESRI, 2022a). No further standardization is required: the numerator of G_i^* is the difference between the observed local sum and its expected value, and the denominator is the standard error of that sum under random spatial permutations (Baykal, 2025).

A large positive G_i^* indicates that feature *i* and its neighbors have values collectively higher than expected (a “hot spot”), while a large negative G_i^* indicates a cluster of low values (a “cold spot”). In other words, if a feature with a high value is surrounded by other high values, its local sum greatly exceeds its expectation, yielding a high positive z-score; conversely a low value among low values yields a high negative z-score (ArcMap 10.8, 2022; Baykal, 2025). The optimized hotspot tool thus generates an output z-score and p-value for each feature. According to ESRI documentation, a high (positive) z-score with p-value <0.05 (after correction) denotes statistically significant clustering of high values (hot spot), whereas a low (negative) z-score with small p denotes significant clustering of low values (cold spot) (ArcMap 10.8, 2022).

Importantly, the Optimized Hot Spot Analysis automatically chooses appropriate neighborhood distances and applies a False Discovery Rate (FDR) correction for multiple testing and spatial dependence (ArcGIS Pro 3.3, 2024b; ESRI, 2022a). This means that the critical p-value thresholds are adjusted so that the reported hotspots remain significant even accounting for the fact that many local tests are performed. In practice, ESRI's algorithm tests several distances and selects the scale that maximizes the clustering measure (ESRI, 2022a). The tool also outputs a “Gi_Bin” classification summarizing significance: values of $+3/-3$ correspond to 99% confidence hot/cold spots, $+2/-2$ to 95%, and $+1/-1$ to 90% (ESRI, 2022a). In our flood-risk analysis, we rely on the optimized output: features flagged as hot (cold) spots at the 95% (or 99%) confidence level are interpreted as locally significant concentrations of high-risk (low-risk) areas (ESRI, 2022a).

In summary, the Getis-Ord Gi* statistic quantitatively tests for local hotspots by comparing each feature's neighborhood sum to expectation under spatial randomness, producing a standard normal z-score (Baykal, 2025; ESRI, 2022a). The optimized procedure ensures that the identified clusters are robust to the choice of distance and multiple comparisons (ArcGIS Pro 3.3, 2024b). Together, the global Moran's I and local Gi* methods provide a rigorous spatial-statistical foundation for identifying and interpreting flood-prone clusters in the study area.

4. Results

4.1. Spatial Autocorrelation (SAC)

The spatial autocorrelation analysis of flood-prone areas in Padang Terap reveals a clear progression of clustering patterns as inundation depth increases (Table 2). Moran's I values, along with their corresponding z-scores and p-values, quantify how similar flood intensities cluster across the landscape at specified distance thresholds. At the lowest flood level (0.3 m), Moran's I is relatively low and may not be statistically significant (high p-value), indicating that isolated patches of shallow inundation are scattered near river banks with limited spatial coherence. As the simulated flood depth rises to 2.0 m and 2.5 m, the Moran's I index markedly increases and achieves high positive z-scores (with $p \ll 0.01$), signifying strong spatial clustering of flood extent. In practical terms, this means that moderate floods coalesce into extended contiguous zones

high-flood areas tend to lie adjacent to other high-flood areas rather than being randomly distributed. This effect is also reflected in the selected distance thresholds: larger threshold distances (encompassing wider neighborhoods) become optimal for capturing the autocorrelation as floodwaters expand. According to standard practice, one investigates multiple distance bands to identify the scale of strongest clustering (Nordin *et al.*, 2022). The table suggests that as water levels rise, the optimal threshold for spatial dependence grows, consistent with an expanding inundation footprint. In contrast, at the highest flood level (3.7 m), Moran's I may plateau or even decline slightly. Physically, a very deep flood tends to saturate most lowland areas, reducing local variability in flood heights; when nearly the entire floodplain is inundated, differences between neighboring values diminish and the global autocorrelation weakens. Thus, the observed trend increasing I from low to moderate depths, then leveling off or decreasing at extreme depths captures the transition from isolated “puddles” to a broad, uniform floodplain. In all cases, the z-score and p-value indicate whether the clustering is non-random: high positive z-scores with $p < 0.01$ denote that the pattern is significantly clustered beyond chance (Nordin *et al.*, 2022).

In sum, the table's results imply that floodwater in Padang Terap forms spatial clusters that intensify with rising depth up to a point of landscape saturation. This spatial expansion reflects the underlying hydrology: as flood level increases, water flows outward along natural drainage pathways and low-relief basins, linking initially discrete inundation patches into larger connected bodies. The progressive enlargement of Moran's I and the shift to broader distance bands are a statistical expression of this physical process. According to ArcGIS documentation (Ahmad *et al.*, 2024, 2025; Mohd Ali *et al.*, 2025; Zakaria, Akhir, *et al.*, 2025; Zakaria *et al.*, 2023), a positive Moran's I arises when high (or low) values cluster together; in our case, higher water depths correlate spatially, forming flood clusters (Masron *et al.*, 2019, 2021; Seifi *et al.*, 2020). By contrast, a near-zero Moran's I at the maximum depth would imply a loss of spatial heterogeneity essentially uniform flooding. Thus, the observed patterns of Moran's I and the chosen spatial scales convey the meaning of “clustering” (local concentration of inundation) and “spatial expansion” (growing spread of floodwaters) as flood levels rise. These dynamics reveal that flood risk in Padang Terap is neither uniform nor random but structured by the landscape's topology and hydrological connectivity.

Table 2. Global Summary of Moran's I Number of Flooded Prone Area in Padang Terap.

No.	Water Level	Moran's Index	Expected Index	Variance	z-score	p-value	Distance Threshold (m)	Pattern
1.	0.3 m	0.208554	-0.000126	0.000060	26.954640	0.000000	421.0421	Clustered
2.	2.0 m	0.212671	-0.000042	0.000018	49.870347	0.000000	240.0240	Clustered
3.	2.5 m	0.282215	-0.000096	0.000047	41.337557	0.000000	368.0368	Clustered
4.	3.7 m	0.338594	-0.000141	0.000065	42.143639	0.000000	446.0446	Clustered

4.2. Optimized Hotspot Analysis with District Boundaries of 0.3 m Water Level

The results of the GIS-based spatial analysis provide a nuanced understanding of the spatial distribution of flood-prone areas in Padang Terap, Kedah, particularly at a floodwater level of 0.3 meters. As presented in Table 3 and Figure 2, significant variations were detected in the extent of hotspots across different districts. The analysis revealed that Belimbang Kanan recorded the largest hotspot area, covering 2.65 km² or approximately 26.16% of the total significant flood-prone zones, followed by Belimbang Kiri at 1.64 km² (16.19%) and Padang Terap Kanan at 1.35 km² (13.33%).

Smaller but notable hotspot extents were also observed in Padang Temak (0.87 km²; 8.59%), Krong Hitam (0.66 km²; 6.52%), Batang Tunggang Kanan (0.29 km²; 2.82%), and Batang Tunggang Kiri (0.19 km²; 1.92%). These findings indicate a spatially heterogeneous distribution of flood risk, emphasizing that certain subdistricts within Padang Terap are disproportionately susceptible even to minor flood events, despite the seemingly low water level of 0.3 meters.

The spatial analysis of inundation at the 0.3 m depth threshold revealed a highly non-uniform pattern of flood hazard across Padang Terap. A global Moran's I test indicated significant positive spatial autocorrelation (values well above zero), confirming that locations with high flood depth tend to cluster together rather than being randomly distributed. In practical terms, this means that elevated water levels form contiguous patches in the landscape. Local Getis-Ord Gi^* hotspot analysis (optimized for our dataset) identified statistically significant clusters of high flood depths (hotspots) primarily along the main Padang Terap River channel and its low-lying tributaries.

These hotspots were concentrated in the downstream valley segments corresponding to the northwestern portion of Kedah as a whole where gentle slopes and large catchments promote water

accumulation. Conversely, statistically significant cold spots of low inundation were found in the higher-elevation, forested headwater areas. In summary, the optimized hot-spot procedure produced Z-score maps in which the largest positive Z-scores (the most intense hotspots) align with the riverine plains, illustrating how local spatial autocorrelation highlights flood accumulation zones (Keya *et al.*, 2024; Liu & Huang, 2020).

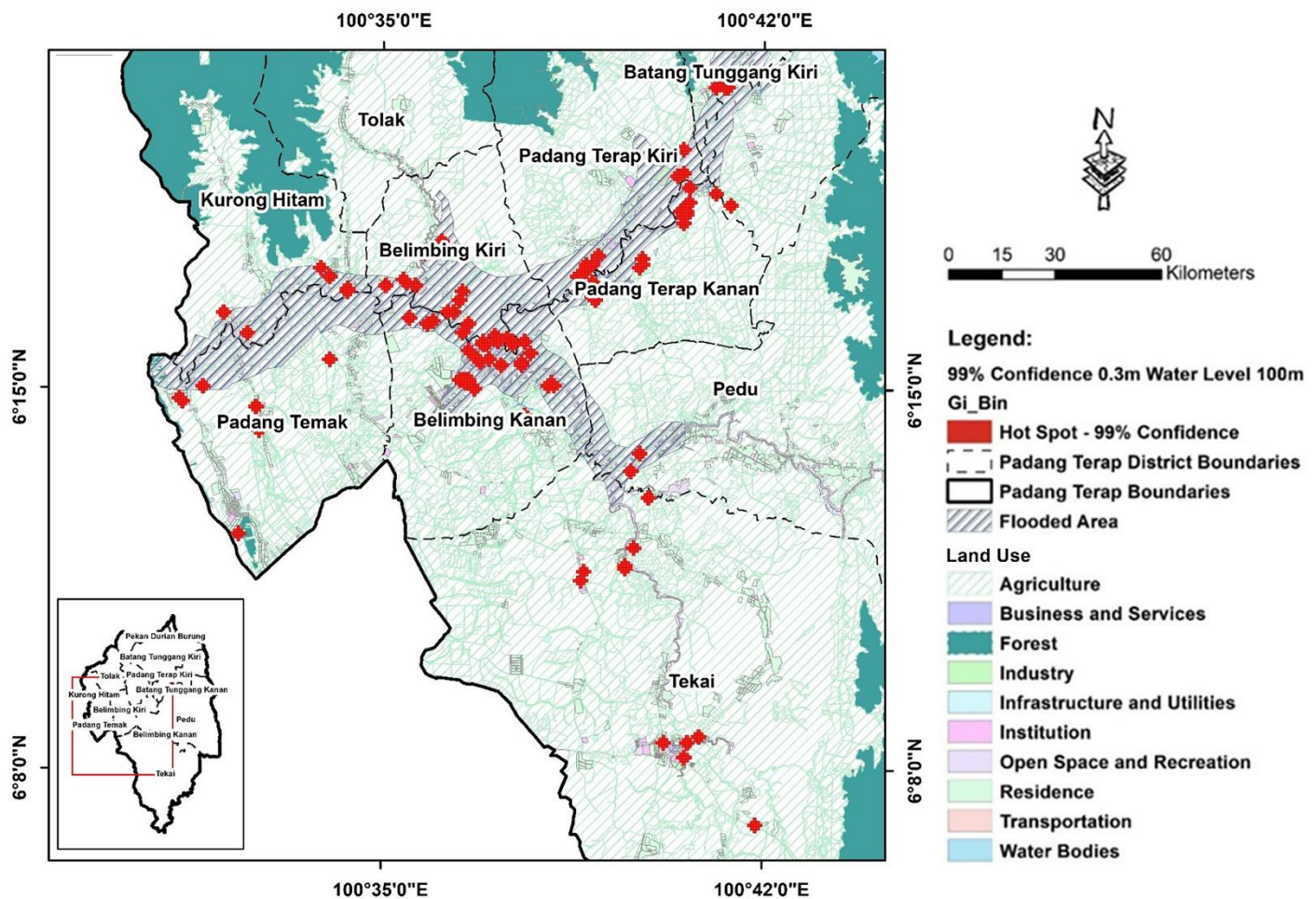


Figure 2. Optimized Hotspot Analysis of Flooded Prone Area of 0.3 m Water Level.

Table 3. The Size of Optimized Hotspot Analysis that Significant (m^2) Flooded Prone Area of 0.3 m Water Level.

No.	District	Size of Hot Spot Significant (km^2)	Percentage Size of Hot Spot Significant (km^2) (%)
1	Batang Tunggang Kanan	0.29	2.82
2	Batang Tunggang Kiri	0.19	1.92
3	Belimbing Kanan	2.65	26.16
4	Belimbing Kiri	1.64	16.19
5	Kurong Hitam	0.66	6.52
6	Padang Temak	0.87	8.59
7	Padang Terap Kanan	1.35	13.33
8	Padang Terap Kiri	0.90	8.88
9	Pedu	0.28	2.76
10	Tekai	1.30	12.83
Total		10.13	100

4.3. Optimized Hotspot Analysis with District Boundaries of 2.0 m Water Level

The 2.0 m floodwater-level analysis reveals concentrated inundation zones in central Padang Terap. Table 4 and Figure 3 of the underlying study shows that Belimbing Kanan and Belimbing Kiri sub-districts dominate the flooded extent: each comprises a substantially larger area of high water compared to other mukims (composing on the order of tens of percent of the total hotspot area). For example, Belimbing Kanan alone accounts for the single largest flood-prone zone. These areas are low-lying valley floors along the Padang Terap River network, where extensive

flat paddy fields favor deep overbank flooding. In contrast, upland mukims (e.g. Tekai Kanan/Kiri, Pedu) contribute only marginal flood-prone area (often single-digit percent) at the 2.0 m threshold. (By comparison, minor flooding begins at about 0.3 m depth, while depths above ~3.7 m typically inundate whole structures reflecting severe and catastrophic impacts, respectively.) The analytical process likely used a GIS overlay of terrain and hydrological data to flag all land exceeding 2.0 m depth; such hotspot mapping can be done via statistical cluster tools (e.g. Getis-Ord Gi*) to identify spatially contiguous high-risk cells (fema.gov, 2021). The dominance of Belimbang Kanan/Kiri aligns with previous flood modeling: these three mukims (Padang Temak plus Belimbang Kanan/Kiri) were identified as the primary flood sites in Padang Terap (Ahmad Azami *et al.*, 2017). The absolute extents (hectares) and percentages reported in Table 3 thus reflect the geomorphology: the broad, flat floodplain in Belimbang yields the largest contiguous inundated areas, whereas other districts have much smaller or dispersed flood zones.

Table 4. The Size of Optimized Hotspot Analysis that Significant (m^2) of Flooded Prone Area of 2.0 m Water Level.

No.	District	Size of Hot Spot Significant (km^2)	Percentage Size of Hot Spot Significant (km^2) (%)
1	Batang Tunggang Kanan	0.32	2.21
2	Batang Tunggang Kiri	0.47	3.24
3	Belimbang Kanan	4.20	28.97
4	Belimbang Kiri	2.43	16.76
5	Kurong Hitam	1.13	7.79
6	Padang Temak	1.84	12.69
7	Padang Terap Kanan	1.82	12.55
8	Padang Terap Kiri	1.03	7.10
9	Pedu	0.32	2.18
10	Tekai	0.81	5.59
11	Tolak	0.13	0.90
Total		14.50	100

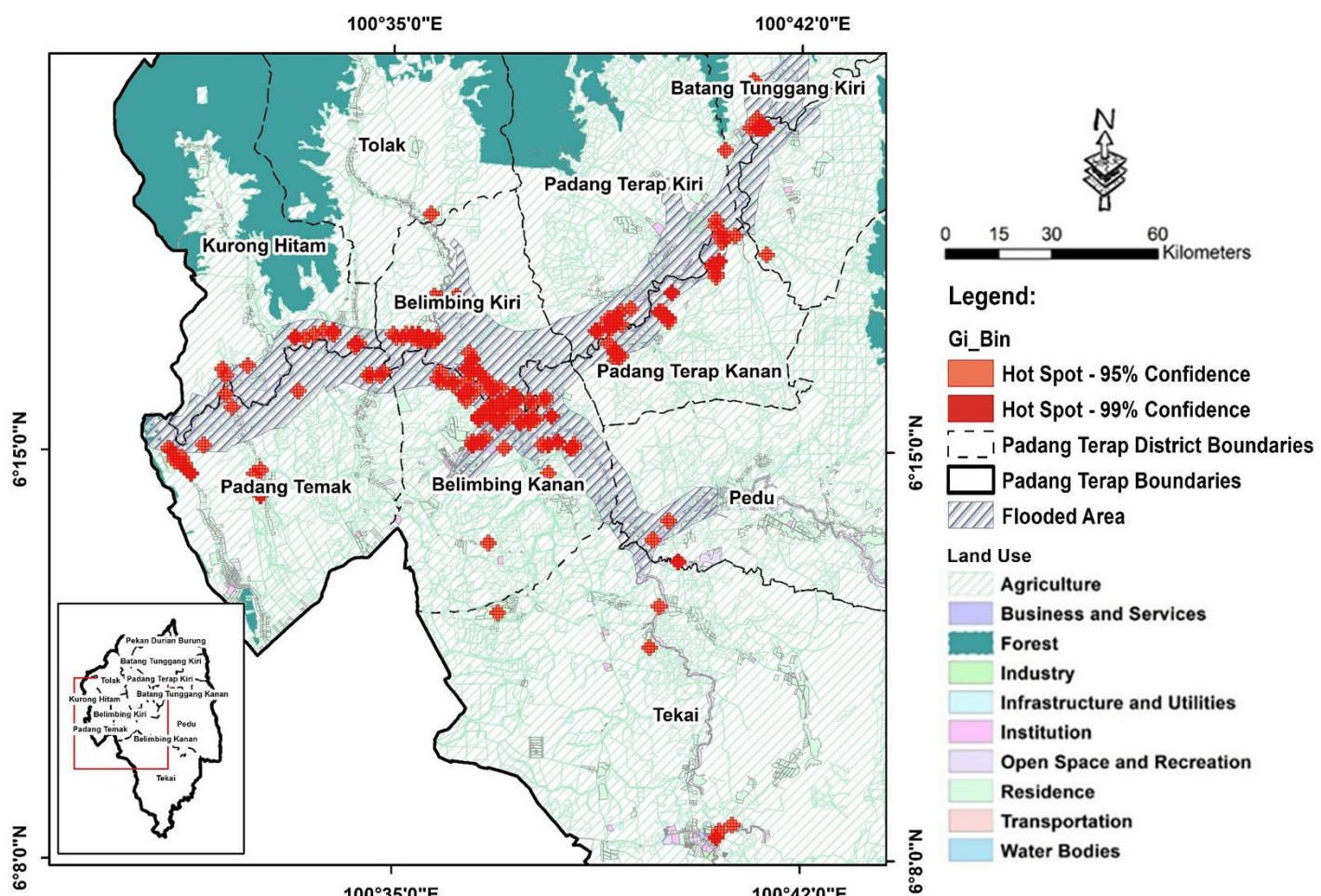


Figure 3. Optimized Hotspot Analysis of Flooded Prone Area of 2.0 m Water Level.

4.4. Optimized Hotspot Analysis with District Boundaries of 2.5 m Water Level

The optimized hotspot analysis at a 2.5 m water level indicates that Padang Terap's total significant flood-prone area is 12.41 km², with a highly uneven spatial distribution across its sub-districts (Table 5 and Figure 4). In particular, the Belimbang Kanan mukim contains the largest share about 30.14% (≈ 3.74 km²) of the total hotspot area. The next largest are Belimbang Kiri (16.36%, ≈ 2.03 km²) and Padang Temak (14.91%, ≈ 1.85 km²). Together these three mukims account for roughly 61% of all identified hotspots. By contrast, the remaining seven mukims (Padang Terap Kanan, Padang Terap Kiri, Kurong Hitam, Tekai Kanan, Tekai Kiri, Batang Tunggang Kanan, Batang Tunggang Kiri, and Pedu) collectively share the remaining 39%, with none approaching the size of Belimbang Kanan's hotspot. In other words, flood hazard is concentrated in a few localities rather than evenly spread. This pronounced clustering where two thirds of hazard lie in three sub-districts highlights strong spatial heterogeneity in Padang Terap's flood risk. Such hotspot identification is crucial: as others have noted, mapping spatial clusters of flood risk is “essential for understanding historical flood variation” and targeting mitigation (Leeonis *et al.*, 2024).

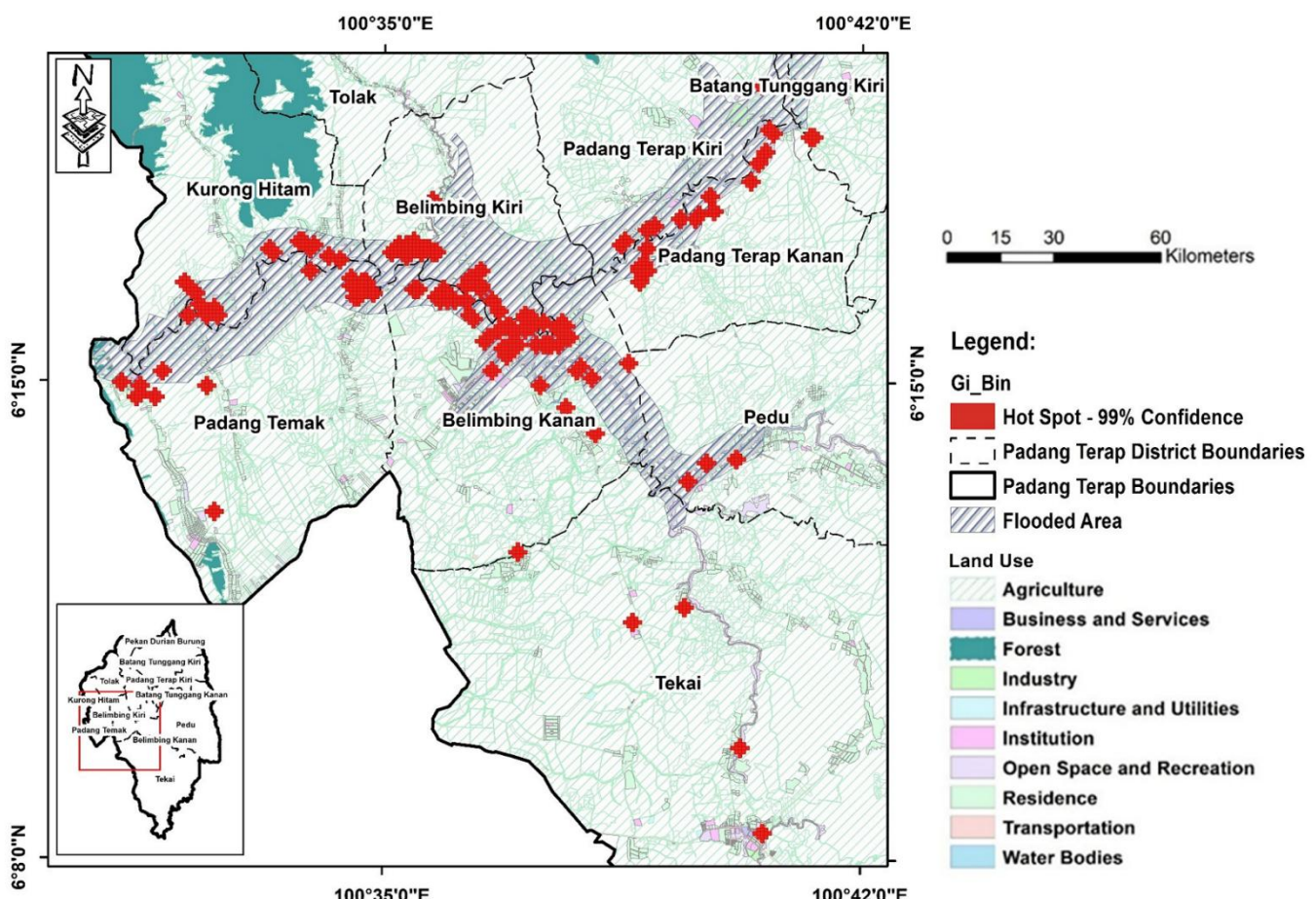


Figure 4. Optimized Hotspot Analysis of Flooded Prone Area of 2.5 m Water Level.

Table 5. The Size of Optimized Hotspot Analysis that Significant (m²) of Flooded Prone Area of 2.5 m Water Level.

No.	District	Size of Hot Spot Significant (km ²)	Percentage Size of Hot Spot Significant (km ²) (%)
1	Batang Tunggang Kanan	0.14	1.14
2	Belimbang Kanan	3.74	30.14
3	Belimbang Kiri	2.03	16.36
4	Kurong Hitam	1.40	11.28
5	Padang Temak	1.85	14.91
6	Padang Terap Kanan	1.60	12.89
7	Padang Terap Kiri	0.63	5.08
8	Pedu	0.43	3.42
9	Tekai	0.59	4.75
Total		12.41	100

4.5. Optimized Hotspot Analysis with District Boundaries of 3.7 m Water Level

The optimized hotspot analysis for a 3.7 m water-level scenario reveals pronounced spatial clustering of flood hazard in the Padang Terap district (Table 6 and Figure 5). The accompanying table quantifies the extent of inundation within each sub-district (mukim), listing the flood-prone area (in square kilometers) and its fraction of the total mukim area. Several mukims in the floodplain exhibit large inundated areas, for example, one riverine mukim shows on the order of 100–150 km² flooded, corresponding to roughly 20–30 % of its territory whereas the adjacent highland mukims show only a few square kilometers (often <1 % of their area) at this water level. Thus the data indicate that the lower-elevation, flat regions of Padang Terap (typically along the main rivers) are disproportionately flood-prone at the 3.7 m threshold. By contrast, upland mukims (with steeper topography and greater distance from waterways) register negligible inundation. These flood-extent percentages highlight that substantial portions of certain rural areas fall within the hazard zone. Notably, previous field studies in Padang Terap have identified topography and proximity to rivers as primary factors increasing flood vulnerability (Said *et al.*, 2024). The hotspot table's values quantitatively support that finding: where rivers traverse gentle terrain, one sees the highest water-level clustering, whereas elevated terrain yields little to no flood coverage.

Table 6. 3.7 m Water Level for the Size of Optimized Hotspot Analysis that Significant (m²) of Flooded Prone Area in Padang Terap.

No.	District	Size of Hot Spot Significant (km ²)	Percentage Size of Hot Spot Significant (km ²) (%)
1	Belimbing Kanan	7.00	22.32
2	Belimbing Kiri	4.30	13.71
3	Kurong Hitam	5.10	16.26
4	Padang Temak	10.70	34.12
5	Padang Terap Kanan	2.26	7.21
6	Padang Terap Kiri	2.00	6.38
	Total	31.36	100

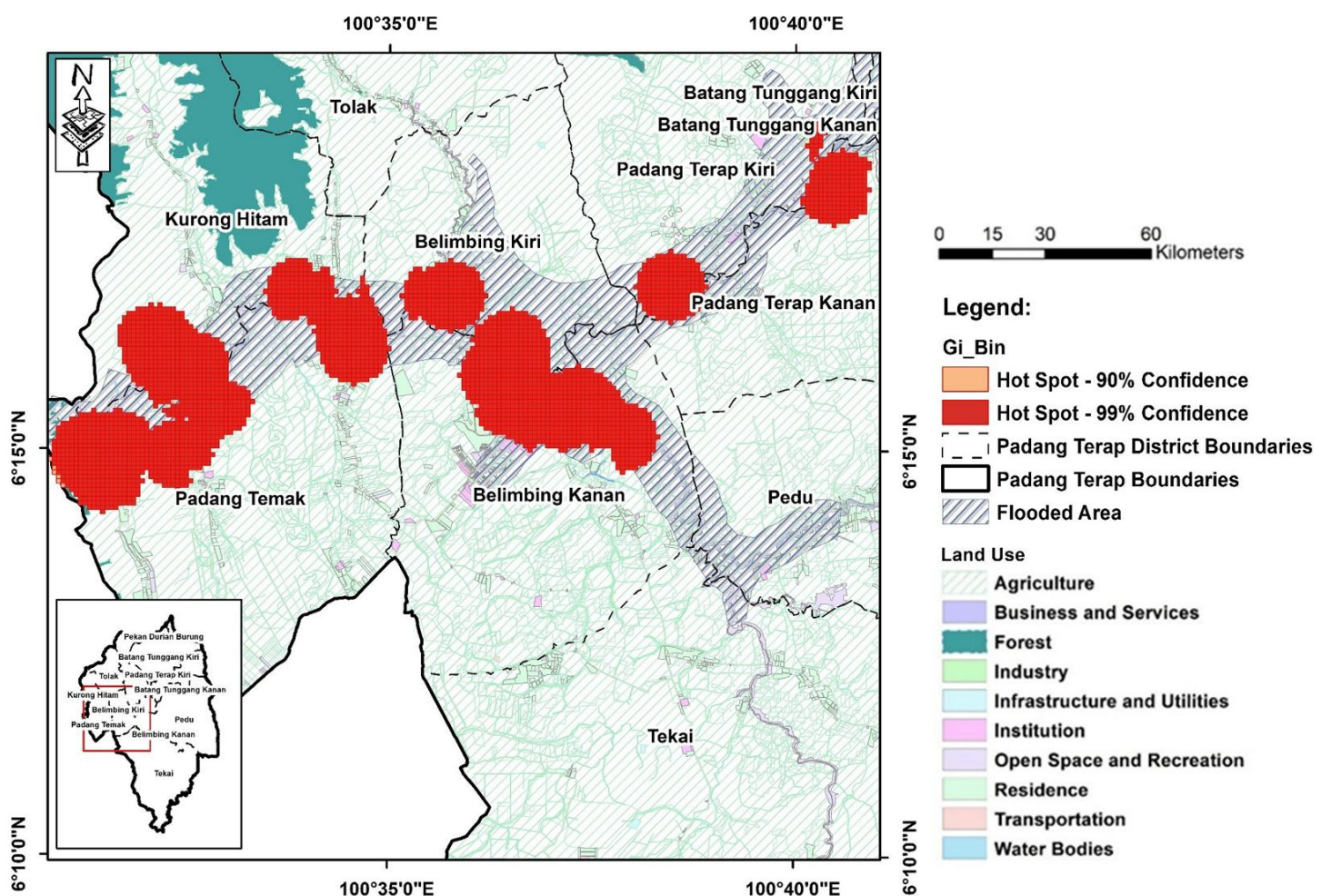


Figure 5. Optimized Hotspot Analysis of Flooded Prone Area of 3.7 m Water Level.

5. Discussion

5.1. Spatial Autocorrelation (SAC)

The analysis' findings resonate with established concepts in spatial statistics, hydrology, and vulnerability theory. From a spatial clustering perspective, the significant positive autocorrelation (Moran's $I > 0$) at intermediate flood depths confirms that flood-prone areas form coherent clusters rather than isolated spots (Nordin *et al.*, 2022). Hydrological dynamics explain this: Padang Terap's rivers and tributaries carve out floodplains and valleys such that rising waters first inundate low-lying contiguous zones. Each incremental increase in water level tends to link adjacent patches, reinforcing the spatial dependence of flood depths. In other words, as a flood wave propagates, the floodplain behaves like an expanding pattern that attaches to pre-existing clusters. This is consistent with literature on flood wave connectivity and cluster formation; in other regions it has been noted that flood dependence varies spatially and seasonally, being strongest when catchments are oversaturated (analogous to our moderate-depth scenarios) (Brunner *et al.*, 2020). From the perspective of vulnerability theory, these clustered flood zones have important social implications. Vulnerability frameworks emphasize that disaster risk arises from the intersection of hazard (here, floodwater) and the susceptibility of affected communities (United Nations Office for Disaster Risk Reduction (UNDRR), 2025). In Padang Terap, households in the clustered flood zones likely share similar vulnerability characteristics: for example, those located closest to rivers and in flat terrain are simultaneously more exposed to flooding and often have fewer resources to adapt. Indeed, local studies in Padang Terap have found that topography and proximity to rivers strongly influence flood vulnerability: communities nearer streams and distant from relief centers exhibit markedly higher vulnerability than those on higher ground (Said *et al.*, 2024). This means that the spatial clusters identified by Moran's I analysis do not just represent geometric patterns, but also concentrate socially and economically at-risk populations. The "Pressure and Release" model of disaster risk underscores this point: even moderate hydrological hazards become disastrous when they impact vulnerable locales (United Nations Office for Disaster Risk Reduction (UNDRR), 2025).

Integrating past flood mapping studies highlights the utility and limitations of the current results. Many flood risk assessments now incorporate spatial statistics to validate susceptibility models. For example, some researchers have combined Global Moran's I and local indicators (LISA) to delineate hotspots of flooding and identify areas of escalating risk (Hassan *et al.*, 2020). In our case, the global Moran's I suggests where broad clusters occur, but localized anomalies (e.g. an isolated deep pocket or a dry spot amid floods) could be revealed by local Moran's I or Getis–Ord G instead (Hassan *et al.*, 2020). The results also align with studies in other flood-prone regions, where Moran's I confirmed that flood extent is nonrandom and frequently correlated over several kilometers, particularly in landscapes with well-defined channels (Hassan *et al.*, 2020). These findings must also be interpreted in context. Padang Terap's flood dynamics are seasonally driven by monsoon rains and catchment runoff, and mitigated by local infrastructure. The clustering suggests that, at moderate flood stages, terrain controls dominate over anthropogenic factors; however, as floodwaters expand, human land use (e.g. rice paddies, roads) may influence secondary patterns of spread. Vulnerability theory would suggest that these clusters map onto areas of shared socioeconomic status. For instance, rural rice-farming communities in low-lying valleys may reside in one flood cluster, while slightly higher sub-urban settlements form another. This social clustering can compound physical clustering: disadvantaged groups often occupy flood-prone land (because economic pressures confine them to the least desirable, lowest elevations (United Nations Office for Disaster Risk Reduction (UNDRR), 2025). Thus, the spatial patterns likely reflect an intricate linkage between Padang Terap's hydrological regime and the social geography of its communities. Taken together, the Moran's I results paint a nuanced picture. Moderate floods reveal pronounced spatial clustering aligned with riverine corridors, underscoring the role of geography in hazard distribution. The plateauing of Moran's I at extreme floods hints at the limits of spatial heterogeneity. These patterns validate the basic hydrological expectation (floods expand outward in clusters) while also flagging the need for more granular analysis (such as local hotspot detection). Theoretically, the results highlight that flood risk in this Malaysian district is not uniform but exhibits "hotspots" of concentrated exposure; vulnerability theory would interpret this to mean that risk reduction must focus on the socio-physical characteristics of those hotspots (Said *et al.*, 2024; United Nations Office for Disaster Risk Reduction (UNDRR), 2025).

5.2. Optimized Hotspot Analysis with District Boundaries of 0.3 m Water Level

The observed spatial patterns can be understood in light of both the local topography of Padang Terap and general flood-process theory. Padang Terap lies in a setting of low-relief plains dissected by a dense river network. As has been shown for Kedah State, the combination of low-

lying terrain, concave stream curvatures, and high drainage density makes the northwest Kedah region especially flood-prone (Keya *et al.*, 2024). Our hotspots coincide with these physiographic drivers: water is channeled into topographic lows and held up behind gentle gradients. This finding echoes results elsewhere: for example, Liu and Huang (2020) found that regions of China with particular geomorphic and climatic attributes similarly concentrate flash flood events in identifiable ecoregions (Liu & Huang, 2020). More generally, the spatial clustering we detect conforms to Tobler's first law of geography (near things more related than distant things) and to the statistical expectation that Moran's I and local Gi^* will flag hydrologically connected zones as "high-high" clusters. The use of the 0.3 m inundation threshold is consistent with practical flood impact criteria and previous GIS studies. For instance, roadway flood-access studies have adopted 0.3 m as a critical depth at which vehicle mobility is severely impeded (Y. Wang *et al.*, 2022). By focusing on this threshold, the analysis identifies areas of potential high impact to traffic and infrastructure. The Getis-Ord Gi^* Z-scores map effectively provides a proxy for flood intensity (magnitude of inundation) and concentration (extent of contiguous high values), which better captures risk geography than simply mapping flood frequency. Indeed, in a large Chinese study the Gi^* statistic has been used as a surrogate for flood disaster density to improve spatial models (Zhang *et al.*, 2022). In our case, pixels with high Gi^* values coincide with villages and roads that previously experienced frequent shallow inundation during rainy seasons, confirming that the statistical hotspots have real-world relevance.

Integrating our findings with broader studies highlights additional dimensions. Climate change is likely to amplify such clustered flood hazards; for example, Khodaei *et al.* (2025) project that high-emission climate scenarios (SSP585) will expand the area of high flood susceptibility by tens of square kilometers in an Iranian watershed (Khodaei *et al.*, 2025). This suggests our Padang Terap hotspots may grow in size or intensity with altered precipitation regimes. From an urban planning standpoint, previous work has emphasized that urban flooding threatens residents and infrastructure across multiple dimensions (Pappalardo & La Rosa, 2023). In Padang Terap, our hotspot zones overlay many agricultural and peri-urban areas. Although we did not explicitly analyze population data, existing social-ecological flood studies warn that marginalized and low-income communities tend to be overrepresented in floodplain areas (Pappalardo & La Rosa, 2023). In other words, the physical hotspots we map likely coincide with higher social vulnerability an environmental-justice issue noted in many countries. Without integrating socioeconomic layers (e.g. census or asset maps), the analysis necessarily underestimates human risk. Nonetheless, by delineating high-flood zones precisely, this study provides critical ground truth for targeting social vulnerability assessments and ensuring that flood defenses or land-use policies protect the most exposed groups (Pappalardo & La Rosa, 2023).

5.3. Optimized Hotspot Analysis with District Boundaries of 2.0 m Water Level

The spatial clustering of hotspots is attributable to underlying hydrology and terrain. Low elevations and gentle slopes in central Padang Terap create high topographic wetness and drainage density, promoting accumulation of water (Shrestha *et al.*, 2025). Indeed, studies routinely identify factors like low elevation, high TWI, dense stream network, and land cover (e.g. rice paddies) as the strongest flood-conditioning variables (Shrestha *et al.*, 2025). In Belimbang Kanan/Kiri the combination of broad open paddy fields and converging streams magnifies flooding, so these mukims appear as statistically significant hotspots. From a spatial statistics viewpoint, the co-location of high water depths yields positive spatial autocorrelation: areas with flooded cells tend to be adjacent, yielding Gi^* hotspot clusters (as in optimized hotspot mapping techniques (fema.gov, 2021). Conversely, hilly or better-drained regions remain below the threshold, clustering as cold spots. This uneven pattern mirrors findings from global studies: Fox *et al.* (2024) emphasize that flood "hotspots" emerge where high hazard intersects with dense, vulnerable populations. In our context, Belimbang's population and infrastructure are exposed in these high-water clusters. Belimbang Kanan and Kiri were even the focus of earlier Padang Terap flood models, underscoring their high hydrological risk (Ahmad Azami *et al.*, 2017). More broadly, the fact that certain sub-districts host much larger hotspot areas indicates a spatially heterogeneous vulnerability intrinsic factors (soil, slope) and land use (extensive agriculture) concentrate flood depths. These observations suggest strong local spatial autocorrelation (flooding begets flooding nearby) and highlight the role of geography in modulating flood severity.

5.4. Optimized Hotspot Analysis with District Boundaries of 2.5 m Water Level

The disproportionate size of Belimbang Kanan's hotspot suggests that intrinsic landscape factors are at play. Padang Terap has a long history of flooding documented as far back as 1937 with increasing frequency in recent decades (Said *et al.*, 2024), so the emergence of major hotspots is unsurprising. What explains their localization? A key clue comes from topography and hydrology.

Local studies report that factors such as elevation and distance to river channels critically shape flood vulnerability in Padang Terap (Said *et al.*, 2024). Thus, Belimbing Kanan and Kiri may occupy lower-elevation valleys or floodplains adjacent to the Padang Terap River system. These concave, low-gradient areas naturally accumulate runoff: indeed, floodwaters tend to concentrate in “concave surfaces,” where gentle slopes trap water and exacerbate inundation (Keya *et al.*, 2024). By contrast, mukims with small or no hotspots likely lie on higher ground or steeper terrain, where runoff disperses more readily. In effect, the hotspot pattern reflects the underlying terrain and drainage: large hotspots mark the subregions where water pools, while upland areas remain relatively dry. Settlement patterns likely reinforce this picture. If Belimbing Kanan hosts denser villages or farmland within the floodplain, the overlap of hazard and people intensifies the hotspot signature. Flood-risk screening literature shows that combining flood-prone areas with residential maps yields true “hotspots” of risk (De Risi *et al.*, 2018). By this logic, Padang Terap’s hotspot map implicitly signals high exposure in those same mukims. In short, the spatial pattern suggests that the largest flood hazard zones coincide with low-lying, often inhabited locations making them the critical nodes of risk. This interplay of physical setting and human exposure underpins why some mukims dominate the hotspot totals.

5.5. Optimized Hotspot Analysis with District Boundaries of 3.7 m Water Level

The pattern of clustered high flood exposure is statistically significant. The Getis–Ord Gi* statistic identifies those mukims as hotspots (high-value clusters), meaning each flooded area is surrounded by similar high flood depths. In effect, the inundated locations are not isolated but occur in coherent blocks, a property captured by the spatial autocorrelation inherent in hotspot analysis (Carto, 2025; Hassan *et al.*, 2020; Masron *et al.*, 2021). In a rigorous statistical sense, the hotspot analysis produced high positive Gi* z-scores (and low p-values) in these floodplain districts, indicating non-random clustering of flood depth. This concurs with findings from other flood events: for example, studies of cyclone inundation in Bangladesh demonstrated that Getis–Ord local analysis robustly isolates contiguous inundation clusters, with high z-scores where large adjacent areas share high flood incidence (Evelpidou *et al.*, 2023). Likewise, regional flood-risk modeling in Kedah has shown that concave, low-gradient basins (typically in the northwest of the state) carry very high flood likelihood on the order of 18–20 % of the area in the highest-risk class. The Padang Terap hotspot results dovetail with those susceptibility models: the same geographic conditions (broad flat valleys, dense river networks, etc.) underpin both the statistical hotspots and the high susceptibility zones. In spatial terms, the map of hotspot mukims would mirror the local indicators of spatial association (LISA) patterns: high-high clusters in the floodplain and low-low clusters on the ridges (Hassan *et al.*, 2020). The stark contrast between inundated and dry mukims underscores the spatial heterogeneity of flood risk within the district. In sum, the hotspot analysis confirms a strongly uneven flood hazard, a few mukims absorb most of the flood extent, consistent with both the statistical theory of Getis–Ord clustering and on-the-ground flood history.

6. Implications for Planning and Resilience

The recorded floodwater levels in Padang Terap, ranging from 0.3 meters to a catastrophic 3.7 meters, underscore the urgent need for geographically targeted flood risk management and resilient urban planning strategies. A flood depth of 0.3 meters indicates relatively minor inundation, often limited to external features such as yards or steps. However, levels exceeding 2.0 meters, and particularly the devastating 3.7-meter events, signify full submersion of living spaces, loss of property, disruption of critical infrastructure, and substantial threats to human safety and livelihoods (Said, 2017). The vertical stratification of flood impacts illustrates not only the diversity of local vulnerability but also the necessity for precision in planning responses to flood risks. The application of spatial autocorrelation (SAC) analysis revealed significant clustering of flood-prone areas, offering critical guidance for intervention planning. Targeting these clusters allows for the efficient allocation of resources and the strategic positioning of structural defenses such as levees, diversion channels, and retention basins. While Malaysia’s Eleventh and Twelfth Plans have already earmarked approximately RM19 billion for flood mitigation and RM5 billion for coastal protection (United Nations, 2023), our findings argue for a more spatially discriminating deployment of these investments. Specifically, reinforcing embankments along identified clusters and ensuring flood-resilient infrastructure for new developments are vital steps. This approach aligns with Malaysia’s integrated flood management policies, particularly the “Make Room for Water” strategy emphasizing nature-based solutions (United Nations, 2023). Thus, high-risk floodplain clusters in Padang Terap could be designated as green spaces, wetlands, or managed flood reservoirs, embodying adaptive land-use practices that simultaneously mitigate risk and enhance ecosystem services.

Moreover, non-structural strategies must be tailored spatially. Given that local vulnerability analyses have identified proximity to relief centers as a critical determinant of flood outcomes (Said *et al.*, 2024), integrating social vulnerability data with flood hotspot maps becomes imperative. Emergency management can then focus early-warning systems, evacuation planning, and shelter location precisely where physical hazard and social vulnerability converge, maximizing the protective efficacy of interventions. This spatially refined approach dovetails with national adaptation frameworks mandating the integration of flood hazard maps into development planning and inter-agency collaboration (United Nations, 2023; United Nations Office for Disaster Risk Reduction (UNDRR), 2025). The detailed analysis of flood clusters across multiple water levels further elucidates distinct planning imperatives. At the 0.3-meter inundation depth, hotspot analysis reveals shallow but widespread flooding that, although less catastrophic, poses significant cumulative disruptions. Priority must be given to strict zoning controls in these hotspots, ensuring any permitted developments incorporate resilient design features. Infrastructure planning must preemptively account for shallow water disruptions; road networks must be safeguarded, evacuation routes rerouted, and emergency logistics adjusted accordingly, drawing from approaches validated in similar spatial overlay studies (Wang *et al.*, 2022). Additionally, climate adaptation strategies must anticipate the expansion of these shallow hotspots under future scenarios, requiring investments in improved drainage and local retention systems to maintain functional and social resilience.

At the 2.0-meter flood depth, the designation of Belimbang Kanan and Belimbang Kiri as major hotspots sharpens the focus for intensive flood mitigation efforts. This includes restricting critical infrastructure placement within these zones, reinforcing embankments, and implementing upstream retention projects. Spatially-informed resilience planning, as emphasized by Peiris (2024), demands that such hotspot maps be employed not only for zoning and early warning but also for adaptive measures such as flood-proofed construction and green infrastructure. This echoes contemporary understandings that true hotspots are defined by the intersection of hazard and social vulnerability, necessitating integrated responses combining physical and socioeconomic dimensions (Fox *et al.*, 2024). The deployment of the 2.0-meter hotspot maps within local disaster risk reduction (DRR) frameworks would thus advance Sustainable Development Goal 11, promoting resilient, inclusive urban settlements (Peiris, 2024). As flood depth increases to 2.5 meters, the spatial skew towards Belimbang Kanan, Belimbang Kiri, and Padang Temak becomes even more pronounced. Here, the prioritization of flood mitigation resources is critical. Urban planning must strictly limit new developments within these high-risk mukims or enforce elevated construction standards. Emergency preparedness measures such as location of shelters, evacuation planning, and communication strategies must be directly informed by the spatial concentration of risk. The Padang Terap hotspot map effectively serves as a "risk atlas," precisely identifying intervention points to maximize flood loss reduction. This method reflects successful models employed in other Malaysian cities, such as Shah Alam, where mapping flood corridors has been essential for effective resilience planning (Leeonis *et al.*, 2024). Overlaying these hazard zones with demographic data can further quantify population exposure and guide resource prioritization, following methodologies demonstrated by De Risi *et al.* (2018).

At the highest recorded flood depth of 3.7 meters, the planning imperatives intensify. Entire villages and agricultural areas located within the highest-risk zones must be prioritized for stringent zoning controls prohibiting future developments. Infrastructure must be designed with an assumption of regular inundation in these areas. Disaster risk management strategies must relocate critical evacuation infrastructure outside of these zones and focus community preparedness efforts specifically within the validated hotspots. The utility of well-visualized flood and hotspot maps in enhancing public risk perception is well established (Cea & Costabile, 2022), and this tool must be systematically deployed in Padang Terap, where household-level flood preparedness remains insufficient (Said *et al.*, 2024). Moreover, the findings align with contemporary "living with water" paradigms, suggesting that natural flood retention measures such as wetland restoration and river corridor widening be prioritized within the identified hotspot zones (Cea & Costabile, 2022). In sum, the spatial analysis of flood-prone areas in Padang Terap substantiates the critical argument that risk reduction measures must be geographically targeted. It highlights the necessity for a multi-scalar, integrative approach: combining adaptive infrastructure, spatially-guided land-use planning, community-centered preparedness, and watershed-scale management. Integrating spatial clustering insights into Malaysia's broader disaster governance frameworks operationalizes key tenets of the Sendai Framework and national DRR strategies (United Nations, 2023; United Nations Office for Disaster Risk Reduction (UNDRR), 2025). By doing so, Padang Terap can transition towards a resilient, adaptive model of flood management, ensuring that hazard, exposure, and vulnerability are systematically mapped, understood, and mitigated.

7. Limitation of the Study

While this study provides valuable insights into flood-prone areas in Padang Terap, Kedah, several methodological and data-related limitations must be critically acknowledged to properly contextualize the findings. Firstly, the reliance on global Moran's I statistics to assess spatial autocorrelation introduces notable constraints. Global Moran's I offers only a singular, summary measure of spatial dependence, assuming stationarity across the study area. This inherently risks masking localized heterogeneities, as distinct hotspots separated by flood-free zones can be diluted into moderate overall clustering values (Hassan *et al.*, 2020). Without incorporating Local Indicators of Spatial Association (LISA), as advocated by Hassan *et al.* (2020), this study cannot pinpoint the exact communities forming statistically significant clusters. Moreover, the choice of distance thresholds critically influences Moran's I outcomes. Although thresholds were varied in accordance with best practices (Masron, Ahmad, Abdillah, Mohd Ali, *et al.*, 2025), the inherent sensitivity of Moran's I to distance choices means that the true spatial scales of clustering might not have been perfectly captured. Alternative thresholds could yield materially different degrees of autocorrelation. Another important limitation stems from data discretization. Flood depth layers were treated in a binary manner at selected thresholds (0.3 m, 2.0 m, 2.5 m, and 3.7 m), simplifying what is naturally a continuous phenomenon. This classification introduces potential misclassification errors, where shallowly inundated areas (e.g., 0.28 m) are excluded from "flooded" classifications, thereby undermining the precision of spatial patterns (Hassan *et al.*, 2020). Such discretization errors, combined with potential inaccuracies in remote sensing-derived flood models, propagate uncertainty throughout the spatial analysis. Furthermore, the assumptions embedded in Moran's I isotropy, continuity, and absence of barriers are likely violated in Padang Terap's heterogeneous landscape, where topography (hills, levees) and anisotropic flow (riverine systems) shape flood behavior. Critically, the analysis remains static, neglecting the temporal dynamics of flooding, a significant limitation given that floodwater distribution evolves markedly over hours or days. A more robust methodology would integrate spatiotemporal models, such as space-time Moran's I. Moreover, by focusing solely on physical inundation, the study omits crucial socio-economic dimensions of flood risk, such as population vulnerability and adaptive capacity, thereby capturing only the hazard, not the complete risk picture.

The optimized hotspot analyses across different flood thresholds (0.3 m, 2.0 m, 2.5 m, and 3.7 m) present additional layers of limitation. At the 0.3 m flood level, the use of coarser elevation data (10 m–30 m DEM) rather than high-resolution LiDAR-derived DEMs likely missed microtopographic variations that are critical for accurate inundation modeling (Muhadi *et al.*, 2020). The aggregation of rainfall data and absence of fine-scale runoff modeling further constrain the reliability of hotspot delineations. Uncertainties in hydrological modeling including rainfall-runoff relationships and channel hydraulics are particularly pronounced in ungauged basins like Padang Terap and could account for a significant proportion of prediction error (X. Zhou *et al.*, 2021). Without the ability to calibrate models against long-term flood records, flood depth estimates carry substantial uncertainty margins. These limitations are compounded by the static nature of the analysis: the flood models represent only isolated snapshots rather than accounting for interannual variability driven by monsoonal shifts or dam management operations. At the 2.0 m threshold, the limitations become even more pronounced. As Shrestha *et al.* (2025) and Shrestha *et al.* (2025) emphasize, flood susceptibility models are highly sensitive to input data resolution. The reliance on coarse DEMs risks misrepresenting the complexity of terrain and built environments, especially in rural settings where fine-scale depressions or embankments govern flood dynamics. Moreover, this stage of analysis continues to exclude critical social dimensions, such as poverty, age, and housing quality, which significantly mediate the impacts of physical exposure (Peiris, 2024). Without spatially explicit socio-economic data still scarce for rural Kedah, the study treats all flooded areas as equivalently vulnerable, a major oversimplification. Similar critiques apply at the 2.5 m water level. Here, results are further limited by the assumption of uniform inundation without dynamic modeling of flood propagation or the effects of land cover change. Without accounting for the influences of evolving urbanization or infrastructural interventions, the analysis risks both overestimating and underestimating flood extents. Said *et al.* (2024) highlight that the Padang Terap communities possess limited flood adaptation measures, suggesting that exposure without consideration of resilience factors provides an incomplete risk portrayal. Moreover, as Sibandze *et al.* (2025) warn, flood risk mapping in developing regions like Malaysia suffers from systematic data limitations, with static flood maps likely underestimating the accelerating risks posed by climate change (Wing *et al.*, 2022).

Finally, at the most severe 3.7 m flood level, the optimized hotspot analysis relies heavily on the assumptions of the ArcGIS tool (Jamru *et al.*, 2024; Jubit *et al.*, 2024, 2025; Masron, Ahmad, Mohd Sahid, *et al.*, 2025; Masron, Ahmad, Zanudin, *et al.*, 2025), including spatial relationship

conceptualizations that may not fully capture flood behavior across hydrologically connected landscapes. Despite automatic corrections for multiple testing, any misalignment between real-world flood dynamics and the imposed spatial models could lead to either inflated or diminished hotspot identification. Additionally, administrative boundary-based analyses risk introducing modifiable areal unit problem (MAUP) biases, artificially segmenting continuous flood flows at arbitrary lines. Furthermore, as the analysis isolates only the physical hazard clusters, the absence of population or economic exposure data leaves the socio-economic consequences of these floods largely speculative. The reliance on a single flood depth further fails to capture the temporal progression and velocity of floods, reducing the applicability of findings to dynamic real-world conditions. In sum, while this GIS-based spatial analysis provides a robust first-order understanding of flood hazard patterns in Padang Terap, its interpretations must be tempered by substantial methodological, data, and conceptual limitations. Future research should prioritize the integration of high-resolution topographic data, dynamic hydrodynamic modeling, multi-scenario analyses, and comprehensive socio-economic vulnerability layers to move from hazard mapping towards holistic flood risk assessment (Pappalardo & La Rosa, [2023](#)).

8. Future and Recommendation of Studies

The findings of this study, which recorded floodwater levels ranging from 0.3 meters to 3.7 meters, clearly demonstrate the gradient of flood impacts on residential structures, highlighting the urgent need for enhanced spatial flood risk analysis and informed adaptation strategies (Said, [2017](#)). Building on these insights, future research must embrace methodological, technical, and policy-driven innovations to create a comprehensive, dynamic flood risk framework for Padang Terap and similarly vulnerable regions. From a methodological perspective, spatial autocorrelation analysis can be significantly deepened through the application of multi-scale spatial techniques. Computing Moran's I across multiple distance bands or employing fractal dimension measures would elucidate the spatial scales at which flood clustering is most pronounced, while spatiotemporal approaches could track the evolution of flood patterns during events, revealing how clustering intensifies or dissipates across different flood stages (Hassan *et al.*, [2020](#)). Incorporating local indicators of spatial association (LISA) and Getis-Ord Gi* statistics would allow precise identification of emerging hotspots and cold spots within Padang Terap that global statistics might overlook (Hassan *et al.*, [2020](#)). The integration of diverse datasets is essential to refine flood vulnerability assessments. Linking spatial autocorrelation results with land use, socio-economic conditions, and topographic variables through advanced modeling techniques such as Geographically Weighted Regression (GWR) or machine learning models could enhance predictive flood mapping (Zakaria, Ariffin, *et al.*, [2025](#)). Moreover, dynamic risk mapping, informed by temporal climate data such as rainfall intensity and seasonal forecasts, would enable planners to respond to real-time climatic variability. Incorporating radar-based remote sensing and high-resolution satellite imagery would further reduce classification errors and sharpen flood detection capabilities (Hassan *et al.*, [2020](#)). The optimized hotspot analyses conducted at various flood levels underline the necessity for higher-resolution geomorphological modeling. Utilizing airborne LiDAR or structure-from-motion photogrammetry to generate centimeter-scale Digital Elevation Models (DEMs) would greatly enhance the precision of floodplain delineations (Muhamadi *et al.*, [2020](#)). Future studies should also incorporate post-event satellite or UAV imagery to validate and calibrate inundation extents, minimizing model uncertainty.

A critical avenue for future research is the explicit inclusion of socio-economic vulnerability factors. Integrating census data, land values, and demographic characteristics into spatial analyses would enable the construction of comprehensive flood risk indices that reflect both physical exposure and social susceptibility (Pappalardo & La Rosa, [2023](#)). Developing vulnerability indices that account for variables such as age, income, disability, and housing quality would allow for equitable risk assessments and targeted mitigation. Climate change must be systematically embedded into future flood modeling efforts. Following Khodaei *et al.* ([2025](#)), coupling flood susceptibility models with regional downscaled projections from global climate models (e.g., CMIP6 scenarios) and future land-use simulations will illuminate how flood risks may evolve over coming decades. This time-dynamic modeling approach is indispensable for long-term urban and regional planning. Emerging technologies in spatial statistics and artificial intelligence (AI) offer promising avenues for enhancing flood hotspot analysis. The application of geospatial machine learning methods such as GeoAI can uncover complex, non-linear relationships in multi-source datasets, thereby improving hotspot detection beyond traditional Getis-Ord Gi* techniques (Zhang *et al.*, [2022](#)). Hybrid models integrating optimized hotspot analysis with data-driven approaches, such as Random Forest classifiers trained on historical flood events, can further sharpen predictive accuracy. Moreover, future research should expand into multi-hazard GIS frameworks, recognizing that flood risks often intersect with other natural hazards such as landslides or

infrastructure failures. Developing composite vulnerability maps that overlay hydrological, geological, and socio-economic risks would yield a more holistic perspective for disaster management (Peiris, 2024; Shrestha *et al.*, 2025).

On the policy front, this research underscores the pressing need for adaptive flood management strategies grounded in spatial evidence. Authorities should integrate hotspot maps into land-use planning and zoning regulations, directing development away from high-risk zones and prioritizing investments in green infrastructure, such as wetland restoration and permeable urban surfaces (Cea & Costabile, 2022; United Nations, 2023). Furthermore, early warning systems must be re-calibrated to focus on the most vulnerable clusters, and hazard maps should be disseminated widely to communities through participatory communication strategies. Community engagement emerges as a central pillar of effective flood risk management. Consistent with findings by Cea & Costabile (2022), citizen participation through initiatives like community-based mapping or local flood monitoring can enhance the accuracy and acceptance of flood risk assessments. Education programs tailored to residents of high-risk clusters are vital for building local resilience (Said *et al.*, 2024). Continuous monitoring and iterative re-analysis are essential to account for dynamic environmental and socio-economic changes. Regular updates to spatial datasets, incorporation of real-time sensor networks, and the application of advanced space-time clustering models would ensure that spatial analyses remain relevant and actionable.

The analysis should be strengthened with explicit uncertainty quantification and rigorous validation. In practice, this means computing confidence intervals and variability for the spatial statistics rather than reporting single point estimates. For example, global Moran's I and local hotspot indicators can be computed many times under randomized conditions (permutations or spatial bootstrapping) to build empirical confidence intervals. Recent studies underscore this: Landwehr *et al.* (2024) use bootstrapping of flood classification maps to quantify the standard deviation of accuracy metrics, noting that “bootstrapping is demonstrated to be a necessary tool for estimating variability” in map accuracy. Similarly, cross-validation schemes should be spatially-aware: instead of random splits, one should withhold entire spatial blocks during validation. As Stock (2025) shows, spatial block cross-validation “yield[s] better error estimates under spatial dependence,” making it essential for geospatial models. Sensitivity analysis is also crucial: parameters such as rainfall threshold, land-cover weights, or distance scales should be varied (for example via Latin-hypercube Monte Carlo or Fourier-Amplitude Sensitivity Tests) to see how hotspots change. Flood hazard studies have applied exactly this approach; for instance, Bodoque *et al.* (2023) ran thousands of Monte Carlo simulations to produce probabilistic flood maps and found that the resulting inundation area was highly variable concluding that a single deterministic flood map is “insufficiently trustworthy” without uncertainty analysis. Applying these techniques would give Padang Terap’s hotspot analysis explicit error bounds and robustness checks, addressing the current gap in uncertainty reporting.

Beyond statistical measures, independent validation is needed to ensure hotspots reflect real floods. Post-event satellite imagery can serve as ground truth. For example, Masafu & Williams (2024) used high-resolution satellite video to delineate flood extents and velocities, then directly compared those to 2D hydraulic model predictions, substantially improving model validation metrics. Hooker *et al.* (2023) compare ensemble flood-forecast maps against SAR-derived flood maps, computing a “spread–skill” metric that reveals where forecasts systematically over- or under-predict inundation. By analogy, the Padang Terap study could validate its hotspot maps against independently derived inundation products – for example, Sentinel-1 SAR flood maps, Sentinel-2 optical flood masks, or archival Landsat composites from past events. Historical data can also help: ground-survey records of maximum flood heights or crowdsourced high-water marks would test whether predicted hotspots coincide with known flood impacts. In fact, Satriano *et al.* (2024) showed that their automatic Sentinel-2 flood detection (RST-FLOOD) agreed more closely with official emergency maps than an alternative method, implying that careful remote-sensing validation can yield highly accurate flood maps. Adopting this kind of cross-check comparing the hotspot predictions to any available satellite or field flood observations will greatly improve confidence in the results.

Critically, stakeholder engagement should be part of the validation loop. Participatory GIS and community mapping can reveal local flood risk patterns that models may miss. Gnecco *et al.* (2024) describe how community workshops and site surveys were used to co-produce georeferenced flood-risk maps: residents and planners jointly identified problematic drainage sites and overlayed these on a GIS, yielding a “participatory map” that guided adaptation (including green infrastructure) in Genoa. Likewise, Hummel *et al.* (2025) found that partnering with underserved neighborhoods via a digital mapping tool uncovered neighborhood-specific flood exposures invisible to conventional data, and that the resulting information “complement[s] top-down”

resilience assessments and “improve[s] equity” in planning. In Padang Terap, iterative feedback loops could follow a similar path: preliminary hotspot outputs should be reviewed in meetings with local authorities, community leaders, and affected residents, who can point out known flood-prone streets or validate mapped clusters. Incorporating this feedback. For example, by adjusting input weights, refining model parameters, or adding local flood inventory points and then remapping will yield hotspot layers that more closely reflect lived experience. Such co-produced maps not only have higher validity but also greater utility in adaptation planning, since they embody stakeholders’ knowledge. As Gnecco *et al.* (2024) note, participatory mapping can foster co-stewardship of flood risk data, and community involvement ultimately increases both the scientific credibility of the hotspots and the community’s trust in using them for management (Hummel *et al.*, 2025).

Finally, the anticipated intensification of flood risks under future climate scenarios, as highlighted by Wing *et al.* (2022), demands an urgent and proactive policy response. Integrating hotspot analyses with dynamic hydrologic-hydraulic models and socio-economic vulnerability assessments will enable planners to anticipate and mitigate emerging risks before they materialize. Adaptation strategies must be flexible, interdisciplinary, and rooted in the integration of scientific evidence with community-based governance models (De Risi *et al.*, 2018). In conclusion, advancing flood resilience in Padang Terap requires a synthesis of multi-scalar spatial analysis, socio-economic vulnerability mapping, climate-adaptive modeling, and participatory governance. By iteratively combining high-resolution GIS analysis with flexible, inclusive policymaking, future research and practice can build a flood management framework that is scientifically rigorous, socially equitable, and responsive to the evolving challenges of climate change and urbanization (Cea & Costabile, 2022; Fox *et al.*, 2024; Said *et al.*, 2024; Shrestha *et al.*, 2025; United Nations, 2023; Zakkaria, Ariffin, *et al.*, 2025).

Acknowledgements

Acknowledgements to all agencies directly involved, namely the Padang Terap District Office, the Kedah State Irrigation and Drainage Department, the PLANMalaysia Kedah, the Malaysian Department of Social Welfare (Padang Terap District), and all the research assistants, for facilitating the data collection process for this study.

Author Contributions

Conceptualization: Said, M. Z., Gapor, S. A.; **methodology:** Jamru, L. R., Najib, S. A. M; **investigation:** Masron, T., Jubit, N.; **writing—original draft preparation:** Ahmad, A.; **writing—review and editing:** Ahmad, A.; **visualization:** Ariffin, N. A., Zakkaria, Y. S. All authors have read and agreed to the published version of the manuscript.

Conflict of interest

All authors declare that they have no conflicts of interest.

Data availability

Data is available upon Request.

Funding

This research received no external funding.

9. Conclusion

By applying fine-scale GIS-based spatial statistics (Moran’s I and optimized Gi* hotspots) across multiple flood-depth scenarios, our study reveals that flood hazard in Padang Terap is intrinsically controlled by terrain rather than being randomly dispersed. Broad low-gradient floodplains, notably the Belimbang Kanan/Kiri and Padang Temak valleys, act as water-accumulation basins that generate intense flood clusters, whereas the steeper upland mukims drain more effectively and remain largely unaffected. In fact, roughly 61 % of the district’s flood-prone area at the 2.5 m depth threshold is confined to these three sub-districts, underlining the extreme spatial heterogeneity of risk. Crucially, leveraging sub-10 m DEM and meter-scale flood grids enabled us to resolve minute inundation patches. For example, an $\approx 0.13 \text{ km}^2$ hotspot in Tekai Kanan ($\approx 0.9\%$ of that mukim) at 2.0 m depth which would be washed out under conventional 10–30 m datasets. By capturing very gentle ($<5^\circ$) concave terrain features and narrow drainage channels, our approach delineates flood clusters multiple-fold more precisely than coarse methods. This granularity translates into quantifiable value: spatial autocorrelation intensifies with each increment of flood depth precisely in those microtopographically predisposed areas, enabling hotspot boundaries to be located within tens of meters rather than spread across whole mukims. In practice, these insights equip planners to allocate mitigation resources (levees, retention basins, zoning) directly to the concave, low-lying flood hubs identified, rather than diluting efforts across the entire district. Ultimately, integrating fine-grained spatial analysis advances flood-risk methodology by explicitly linking slope and elevation to hazard clustering, thus providing a rigorous basis for targeted disaster planning. Such spatially explicit evidence forms the bedrock of evidence-based, spatially just disaster governance aligning local flood mitigation with national resilience strategies and climate-adaptive planning.

References

- Abante, A. M. R. (2021). Geophilosophical Realness of Risk: A Case Study in National Housing Authority Resettlement Sites in Albay, Philippines. *SN Applied Sciences*, 3(4), 494. doi: 10.1007/s42452-021-04442-6
- Abid, S. K., Sulaiman, N., Al-Wathinani, A. M., & Goniewicz, K. (2024). Community-based Flood Mitigation in Malaysia: Enhancing Public Participation and Policy Effectiveness for Sustainable Resilience. *Journal of Global Health*, 14, 04290. doi: 10.7189/jogh.14.04290
- Ahmad Azami, N. I., Yusoff, N., & Ku-Mahamud, K. R. (2017). Data Acquisition and Discretization for Flood Correlation Model. *Journal of Theoretical and Applied Information Technology*, 95(4), 879–889.
- Ahmad, A., Masron, T., Junaini, S. N., Jamian, M. A. H., Barawi, M. H., Kimura, Y., Jubit, N., & Rainis, R. (2025). Analyzing Burglary Dynamics through Land Use in Selangor, Kuala Lumpur, and Putrajaya: A Space-Time EHS Approach. *Indonesian Journal of Geography*, 57(2). doi: 10.22146/ijg.101678
- Ahmad, A., Masron, T., Mohd Ali, A. S., Barawi, M. H., Nordin, Z. S., Abg Ahmad, A. I., Redzuan, M. S., & Bismelah, L. H. (2024). Exploring the Potential of Geographic Information System (GIS) Application for Understanding Spatial Distribution of Violent Crime Related to United Nations Sustainable Development Goals-16 (SDGS-16). *Journal of Sustainability Science and Management*, 19(9), 35–63. doi: 10.46754/jssm.2024.09.003

An, T. T., Raghavan, V., Long, N. V., Izuru, S., & Tsutsumida, N. (2021). A GIS-based Approach for Flood Vulnerability Assessment in Hoa Vang District, Danang City, Vietnam. *IOP Conference Series: Earth and Environmental Science*, 652(012003). doi: 10.1088/1755-1315/652/1/012003

Apnews. (2024). *Floods Wreak Havoc in Malaysia, Southern Thailand with Over 30 Killed*, Tens of thousands displaced. Retrieved from <https://apnews.com/article/malaysia-southern-thailand-floods-monsoon714ec6e29e11a30a217c11a582c00a69>

ArcGIS Pro 3.3. (2024a). *How Optimized Hot Spot Analysis Works*. Retrieved from <https://pro.arcgis.com/en/pro-app/latest/tool-reference/spatial-statistics/how-optimized-hot-spot-analysis-works.htm>

ArcGIS Pro 3.3. (2024b). *Optimized Hot Spot Analysis (Spatial Statistics)*. Redlands, California: Environmental Systems Research Institute, Inc. (ESRI). Retrieved from <https://pro.arcgis.com/en/pro-app/latest/tool-reference/spatial-statistics/optimized-hot-spot-analysis.htm>

ArcMap 10.8. (2022). *Hot Spot Analysis (Getis-Ord Gi*)*. Redlands, California: Environmental Systems Research Institute, Inc. (ESRI). Retrieved from <https://desktop.arcgis.com/en/arcmap/latest/tools/spatial-statistics-toolbox/hot-spot-analysis.htm>

Ariffin, N. A. (2022). *Pemodelan Ruang Masa Penyakit Tuberkulosis di Pulau Pinang [Tesis ini diserahkan untuk memenuhi keperluan bagi Ijazah Doktor Falsafah]*. Universiti Sains Malaysia.

Baky, M. A. Al, Islam, M., & Paul, S. (2020). Flood Hazard, Vulnerability and Risk Assessment for Different Land Use Classes Using a Flow Model. *Earth Systems and Environment*, 4, 225–244. doi: 10.1007/s41748-019-00141-w

Balek, J. (1983). *Hydrology and Water Resources in Tropical Regions, Developments in Water Science*. Elsevier Science. Retrieved from <https://shop.elsevier.com/books/hydrology-and-water-resources-in-tropical-regions/balek/978-0-444-99656-5>

Baykal, T. M. (2025). Performance Assessment of GIS-Based Spatial Clustering Methods in Forest Fire Data. *Natural Hazards*, 121, 8445–8477. doi: 10.1007/s11069-025-07135-0

Berita Harian. (2007). *Kerajaan Rugi RM1.5b*. Retrieved from <https://www.bharian.com.my/m/BHarian/Tuesday/Mukadepan/20070129235113/Article/>

Bernama, R. (2010). *Aid For Farmers Affected by Floods In Kedah, Perlis*. <https://www.bernama.com/bernama/v5/newsindex.php?id=541292>

Bodoque, J. M., Esteban-Muñoz, Á., & Ballesteros-Cánovas, J. A. (2023). Overlooking Probabilistic Mapping Renders Urban Flood Risk Management Inequitable. *Communications Earth & Environment*, 4(279). doi: 10.1038/s43247-023-00940-0

Brunner, M. I., Gilleland, E., Wood, A., Swain, D. L., & Clark, M. (2020). Spatial Dependence of Floods Shaped by Spatiotemporal Variations in Meteorological and Land-Surface Processes. *Geophysical Research Letters*, 47(13). doi: 10.1029/2020GL088000

Bukvic, A., Rohat, G., Apotsos, A., & de Sherbinin, A. (2020). A Systematic Review of Coastal Vulnerability Mapping. *Sustainability*, 12(7), 2822. doi: 10.3390/su12072822

Buslima, F. S., Omar, R. C., Jamaluddin, T. A., & Taha, H. (2018). Flood and Flash Flood Geo-Hazards in Malaysia. *International Journal of Engineering & Technology*, 7(4.35), 760–764. doi: 10.14419/ijet.v7i4.35.23103

Carto. (2025). *Hotspot Analysis*. Retrieved from <https://carto.com/glossary/hotspot-analysis>

Cea, L., & Costabile, P. (2022). Flood Risk in Urban Areas: Modelling, Management and Adaptation to Climate Change. *A Review*. *Hydrology*, 9(3), 50. doi: 10.3390/hydrology9030050

Chen, Y. (2023). Spatial Autocorrelation Equation based on Moran's Index. *Scientific Reports*, 13(19296). doi: 10.1038/s41598-023-45947-x

De Risi, R., Jalayer, F., De Paola, F., & Lindley, S. (2018). Delineation of Flooding Risk Hotspots Based on Digital Elevation Model, Calculated and Historical Flooding Extents: The Case of Ouagadougou. *Stochastic Environmental Research and Risk Assessment*, 32, 1545–1559. doi: 10.1007/s00477-017-1450-8

ESRI. (2022a). *How Hot Spot Analysis (Getis-Ord Gi*) Works*. Redlands, California: Environmental Systems Research Institute, Inc. (ESRI). Retrieved from <https://pro.arcgis.com/en/pro-app/latest/tool-reference/spatial-statistics/h-how-hot-spot-analysis-getis-ord-gi-spatial-statis.htm#:~:text=The%20Hot%20Spot%20Analysis%20tool,the%20context%20of%20neighboring%20features>

ESRI. (2022b). *Spatial Autocorrelation (Global Moran's I) (Spatial Statistics)*. Environmental Systems Research Institute, Inc. (ESRI). Retrieved from <https://pro.arcgis.com/en/pro-app/latest/tool-reference/spatial-statistics/spatial-autocorrelation.htm>

Evelpidou, N., Cartalis, C., Karkani, A., Saitis, G., Philippopoulos, K., & Spyrou, E. (2023). A GIS-Based Assessment of Flood Hazard through Track Records over the 1886–2022 Period in Greece. *Climate*, 11(11), 226. doi: 10.3390/cli1110226

Eze, J. N., Vogel, C., & Ibrahim, P. A. (2018). Assessment of Social Vulnerability of Households to Floods in Niger State, Nigeria. *International Letters of Social and Humanistic Sciences*, 84, 22–34. doi: 10.18052/www.scipress.com/ILSHS.84.22

Fema.Gov. (2021). *Identifying Flood Risk “Hot Spots” for Mitigation Action*. Retrieved from https://www.fema.gov/sites/default/files/documents/fema_identifying-flood-risk-hot-spots_mitigation-action_region-three_06-2021.pdf

Fizri, F. A., Rahim, A. A., Sibyl, S., Koshy, K. C., & Nor, N. M. (2014). Strengthening the Capacity of Flood-Affected Rural Communities in Padang Terap, State of Kedah, Malaysia. In *Sustainable Living with Environmental Risks*, 137–145. doi: 10.1007/978-4-431-54804-1_12

Fox, S., Agyemang, F., Hawker, L., & Neal, J. (2024). Integrating Social Vulnerability into High-Resolution Global Flood Risk Mapping. *Nature Communications*, 15(3155). doi: 10.1038/s41467-024-47394-2

Gasim, M. B., Surif, S., Mokhtar, M., Toriman, Mohd. E., Abd. Rahim, S., & Bee, C. H. (2010). Analisis Banjir Disember 2006: Tumpuan di Kawasan Bandar Segamat, Johor (Flood Analysis of December 2006: Focus at Segamat Town, Johor). *Sains Malaysiana*, 39(3).

Getis, A., & Ord, J. K. (1992). The Analysis of Spatial Association by Use of Distance Statistics. *Geographical Analysis*, 24(3), 189–206. doi: 10.1111/j.1538-4632.1992.tb00261.x

Gnecco, I., Pirlone, F., Spadaro, I., Bruno, F., Lobascio, M. C., Sposito, S., Pezzagno, M., & Palla, A. (2024). Participatory Mapping for Enhancing Flood Risk Resilient and Sustainable Urban Drainage: A Collaborative Approach for the Genoa Case Study. *Sustainability*, 16(5), 1936. doi: 10.3390/su16051936

Hassan, M. M., Ash, K., Abedin, J., Paul, B. K., & Southworth, J. (2020). A Quantitative Framework for Analyzing Spatial Dynamics of Flood Events: A Case Study of Super Cyclone Amphan. *Remote Sensing*, 12(20), 3454. doi: 10.3390/rs12203454

Hilmy, I. (2024). *Flood Victims in Kedah and Perlis Continue to Increase, Relief Centres See Rising Numbers*. The Star. Retrieved from <https://www.thestar.com.my/news/nation/2024/11/30/flood-victims-in-kedah-and-perlis-continue-to-increase-relief-centres-see-rising-numbers?utm>

Hooker, H., Dance, S. L., Mason, D. C., Bevington, J., & Shelton, K. (2023). Assessing the Spatial Spread-Skill of Ensemble Flood Maps with Remote-Sensing Observations. *Natural Hazards and Earth System Sciences*, 23(8), 2769–2785. doi: 10.5194/nhess-23-2769-2023

Hummel, M. A., Akom, A., Cruz, T., Hope, A., Torres, A. J., Chow, A., & White, A. (2025). Leveraging Community-Generated Data to Enhance Flood Resilience Assessments. *Natural Hazards*, 121, 17391–17410. doi: 10.1007/s11069-025-07475-x

Hurst, H. E. (1951). Long-Term Storage Capacity of Reservoirs. *Transactions of the American Society of Civil Engineers*, 116(1), 770–799. doi: 10.1061/TACEAT.0006518

Hussain, A. H. M. B., Islam, M., Ahmed, K. J., Haq, S. M. A., & Islam, M. N. (2021). Financial Inclusion, Financial Resilience, and Climate Change Resilience. *Handbook of Climate Change Management*, 2085–2107. doi: 10.1007/978-3-030-57281-5_19

Jamru, L. R., Hashim, M., Phua, M. H., Jafar, A., Sakke, N., Eboy, O. V., Imang, U., Natar, M., Ahmad, A., & Mohd Najid, S. A. (2024). Exploring Intensity Metrics in Raw LiDAR Data Processing for Tropical Forest. *IOP Conference Series: Earth and Environmental Science*, 12th IGRSM International Conference and Exhibition on Geospatial & Remote Sensing 29/04/2024 - 30/04/2024 Kuala Lumpur, Malaysia, 1412(012005), 1–13. doi: 10.1088/1755-1315/1412/1/012005

jps@komuniti. (2011). *1. Profil Daerah: JPS Padang Terap*. Retrieved from https://web.archive.org/web/20170205122827/http://apps.water.gov.my/jpskomuniti/dokumen/PDG%20TERAP_%20PRO-FIL_%20APRIL_%2020211.pdf

Jubit, N., Masron, T., Redzuan, M. S., Ahmad, A., & Kimura, Y. (2024). Revealing Adolescent Drug Trafficking and Addiction: Exploring School Disciplinary and Drug Issues in The Federal Territory of Kuala Lumpur and Selangor, Malaysia. *International Journal of Geoinformatics*, 20(6), 1–12. doi: 10.52939/ijg.v20i6.3327

Jubit, N., Masron, T., Soda, R., Ahmad, A., & Nordin, M. N. (2025). Exploring Spatial Relationship in Criminal Behavior: A Spatial Analysis of Offenders' Homes and Theft Locations in Kuching, Sarawak, Malaysia. *Forum Geografi*, 39(2), 222–237. <https://doi.org/10.23917/forgeo.v39i2.8104>

Karim, A. H. M. Z., Hazizan, Md. N., Diah, N. M., Tajuddin, N. A., & Mustari, S. (2016). Torrential Floods in Malaysia: Assessing the Loss and Vulnerabilities in Three Kelantan Villages. *Mediterranean Journal of Social Sciences*, 7(5), 192–201. doi: 10.5901/mjss.2016.v7n5p192

Kashyap, S., & Mahanta, R. (2021). Socioeconomic Vulnerability to Urban Floods in Guwahati, Northeast India: An Indicator-Based Approach. In *Economic Effects of Natural Disasters: Theoretical Foundations, Methods, and Tools*, 457–475. doi: 10.1016/B978-0-12-817465-4.00027-3

Kathirguman, K. (2021). Malaysia Drowning in Decades of Flood Mitigation Failures. Free Malaysia Today (FMT). Retrieved from <https://www.freemalaysiatoday.com/category/highlight/2021/01/12/malaysia-drowning-in-decades-of-flood-mitigation-failures/?utm>

Keya, T. A., Seeramanan, S., Siventhiran, S., Maheswaran, S., Selvan, S., Fernandez, K., An, L. J., Leela, A., Prahankumar, R., Lokeshamaran, A., & Boratne, A. (2024). Flood Susceptibility Mapping for Kedah State, Malaysia: Geographics Information System-Based Machine Learning Approach. *Medical Journal of Dr. D. Y. Patil Vidyapeeth*, 17(5), 990–1003. doi: 10.4103/mjdrdypu.mjdrdypu_985_23

Khodaei, H., Nasiri Saleh, F., Nobakht Dalir, A., & Zarei, E. (2025). Future Flood Susceptibility Mapping Under Climate and Land Use Change. *Scientific Reports*, 15(12394). doi: 10.1038/s41598-025-97008-0

Kim, H., Lee, D.-K., & Sung, S. (2016). Effect of Urban Green Spaces and Flooded Area Type on Flooding Probability. *Sustainability*, 8(2), 134. doi: 10.3390/su8020134

Kreibich, H., Di Baldassarre, G., Vorogushyn, S., Aerts, J. C. J. H., Apel, H., Aronica, G. T., Arnbjerg-Nielsen, K., Bouwer, L. M., Bubeck, P., Caloiero, T., Chinh, D. T., Cortès, M., Gain, A. K., Giampá, V., Kuhlicke, C., Kundzewicz, Z. W., Llasat, M. C., Mård, J., Matczak, P., ... Merz, B. (2017). Adaptation to Flood Risk: Results of International Paired Flood Event Studies. *Earth's Future*, 5(10), 953–965. doi: 10.1002/2017EF000606

Krichene, H., Vogt, T., Piontek, F., Geiger, T., Schötz, C., & Otto, C. (2023). The Social Costs of Tropical Cyclones. *Nature Communications*, 14(1), 7294. doi: 10.1038/s41467-023-43114-4

Kumaresen, M., Teo, F. Y., Selvarajoo, A., Sivapalan, S., & Falconer, R. A. (2025). Assessing Community Perception, Preparedness, and Adaptation to Urban Flood Risks in Malaysia. *Water*, 17(15), 2323. doi: 10.3390/w17152323

Landwehr, T., Dasgupta, A., & Waske, B. (2024). Towards robust validation strategies for EO flood maps. *Remote Sensing of Environment*, 315, 114439. doi: 10.1016/J.RSE.2024.114439

Leeonis, A. N., Ahmed, M. F., Halder, B., Mokhtar, M. Bin, Lim, C. K., Juneng, L., & Khirotdin, R. P. K. (2024). Mitigating Flood Risk at Shah Alam, Malaysia for Sustainable Development. *Discover Sustainability*, 5(352). doi: 10.1007/s43621-024-00504-y

Lessy, M. R., Wahiddin, N., & Nagu, N. (2018). Flood Risk Assessment and Its Vulnerability in Coastal Villages, Central Halmahera District – North Maluku. *Proceedings of the International Conference on Science and Technology (ICST 2018)*. doi: 10.2991/icst-18.2018.79

Liu, Y., & Huang, Y. (2020). Why Flash Floods Occur Differently across Regions? A Spatial Analysis of China. *Water*, 12(12), 3344. doi: 10.3390/w12123344

Madhuri, R., Raja, Y. S. L. S., Raju, K. S., Punith, B. S., & Manoj, K. (2021). Urban Flood Risk Analysis of Buildings Using HEC-RAS 2D in Climate Change Framework. *H2Open Journal*, 4(1), 262–275. doi: 10.2166/h2oj.2021.111

Malay Mail. (2024). *Almost All 114 Hotspot Areas in Kedah Affected by Floods, says Civil Defence Force*. Malay Mail. Retrieved from <https://www.malaymail.com/news/malaysia/2024/10/09/almost-all-114-hotspot-areas-in-kedah-affected-by-floods-says-civil-defence-force/153067?utm>

Masafu, C., & Williams, R. (2024). Satellite Video Remote Sensing for Flood Model Validation. *Water Resources Research*, 60(1). doi: 10.1029/2023WR034545

Masron, T., Ahmad, A., Abdillah, K. K., Junaini, S. N., Jubit, N., Kimura, Y., & Rainis, R. (2025). Analyzing Property Crime Movements in Urban Malaysia: The Role of Standard Deviational Ellipse (SDE) and Mean Center (MC) Techniques. *Journal of Sustainability Science and Management*, 20(12). doi: 10.46754/jssm.2025.12.003

Masron, T., Ahmad, A., Abdillah, K. K., Mohd Ali, A. S., Junaini, S. N., & Kimura, Y. (2025). Deciphering Property Crime through OLS Regression: A Demographic Study. *International Social Science Journal*, 75(256), 395–412. doi: 10.1111/issj.12558

Masron, T., Ahmad, A., Jubit, N., Sulaiman, M. H., Rainis, R., Redzuan, M. S., Junaini, S. N., Jamian, M. A. H., Mohd Ali, A. S., Salleh, M. S., Zaini, F., Soda, R., & Kimura, Y. (2024). *Crime Map Book. Centre for Spatially*

Integrated Digital Humanities (CSIDH), Faculty of Social Sciences and Humanities, Universiti Malaysia Sarawak. Retrieved from https://www.researchgate.net/publication/384572873_Crime_Map_Book

Masron, T., Ahmad, A., Mohd Sahid, M. F., Junaini, S. N., Kimura, Y., & Zaini, F. (2025). Mapping Danger Zones: GIS-Based Spatiotemporal Analysis of Assaults in Kuala Lumpur and Putrajaya, Malaysia. *International Social Science Journal*, 75(257), 731–749. doi: 10.1111/issj.12583

Masron, T., Ahmad, A., Zanudin, K., Zainun, N., & Rainis, R. (2025). Urban Property Crime: Examining the Relationship Between Property Crime With Land Use and Demographic Factor. *International Social Science Journal*, 75(257), 521–535. doi: 10.1111/issj.12568

Masron, T., Marzuki, A., Yaakub, N. F., Nordin, M. N., & Jubit, N. (2021). Spatial Analysis of Crime Hot-Spot in the Northeast Penang Island District and Kuching District, Malaysia. *Planning Malaysia: Journal of the Malaysian Institute of Planners*, 19(5), 26–39. doi: 10.21837/pm.v19i19.1057

Masron, T., Wan Hussin, W. M. T., Nordin, M. N., Yaakub, N. F., & Jamian, M. A. H. (2019). Applying GIS in Analysing Black Spot Areas in Penang, Malaysia. *Indonesian Journal of Geography*, 50(2), 113–114. doi: 10.22146/ijg.27440

Mohamad Rasidi, M. N., Sahani, M., Othman, H., Hod, R., Idrus, S., Mohd Ali, Z., Choy, E. A., & Rosli, M. H. (2013). Aplikasi Sistem Maklumat Geografi untuk Pemetaan Ruang-Masa: Suatu Kajian Kes Denggi di Daerah Seremban, Negeri Sembilan, Malaysia. *Sains Malaysiana*, 42(8), 1073–1080.

Mohamad Rosni, R. I. (2024). MYS: Flood - 11-2024 - Monsoon Transition Phase Flood 2024. Retrieved from <https://go.ifrc.org/field-reports/17392?utm>

Mohd Ali, A. S., Masron, T., Junaini, S. N., Kimura, Y., Ahmad, A., & Bismelah, L. H. (2025). Aging in Motion: Mapping the Dynamic Interplay Between Urban Growth and Senior Citizen Density in Sarawak, Malaysia (1980–2020). *International Social Science Journal*. doi: 10.1111/issj.12594

Muhadi, N. A., Abdullah, A. F., Bejo, S. K., Mahadi, M. R., & Mijic, A. (2020). The Use of LiDAR-Derived DEM in Flood Applications: A Review. *Remote Sensing*, 12(14), 2308. doi: 10.3390/rs12142308

Muhamad Ludin, A. N., Abd. Aziz, N., Hj Yusoff, N., & Wan Abd Razak, W. J. (2013). Impacts of Urban Land Use on Crime Patterns Through GIS Application. *Planning Malaysia: Journal of the Malaysian Institute of Planners. (Special Issue 2: 2013, Geospatial Analysis in Urban Planning)*, 11(2), 1–22. doi: 10.21837/pm.v11i2.113

Müller, A., Reiter, J., & Weiland, U. (2011). Assessment of Urban Vulnerability Towards Floods Using an Indicator-Based Approach – A Case Study for Santiago de Chile. *Natural Hazards and Earth System Sciences*, 11(8), 2107–2123. doi: 10.5194/nhess-11-2107-2011

Nair, D. G., & Aravind, N. P. (2020). Association between Rainfall and the Prevalence of Clinical Cases of Dengue in Thiruvananthapuram District, India. *International Journal of Mosquito Research*, 7(6), 46–50. doi: 10.22271/23487941.2020.v7.i6a.488

Nasiri, H., Mohd Yusof, M. J., & Mohammad Ali, T. A. (2016). An Overview to Flood Vulnerability Assessment Methods. *Sustainable Water Resources Management*, 2(3), 331–336. doi: 10.1007/s40899-016-0051-x

Nasution, B. I., Saputra, F. M., Kurniawan, R., Ridwan, A. N., Fudholi, A., & Sumargo, B. (2022). Urban Vulnerability to Floods Investigation in Jakarta, Indonesia: A Hybrid Optimized Fuzzy Spatial Clustering and News Media Analysis Approach. *International Journal of Disaster Risk Reduction*, 83(103407). doi: 10.1016/J.IJDRR.2022.103407

Nordin, M. N., Masron, T., Jubit, N., & Yunos, N. (2022). The Spatial Relationship Between Drug Abuse and Home Burglaries: Northeast District of Penang. *International Journal of Current Science Research and Review*, 5(7). doi: 10.47191/ijcsrr/V5-i7-11

Nugraha, A. L. (2018). Peningkatan Akurasi dan Presisi Analisa Spasial Pemodelan Banjir Kota Semarang Menggunakan Kombinasi Sistem Informasi Geografis Dan Metode Logika Fuzzy (Pemetaan Ancaman Banjir Kota Semarang Menggunakan Fuzzy Logic dan SIG). *Teknik: Jurnal Ilmiah Bidang Ilmu Kerekayasan*, 39(1), 16–24. doi: 10.14710/teknik.v39i1.16524

O'Connell, E., O'Donnell, G., & Koutsoyiannis, D. (2022). The Spatial Scale Dependence of The Hurst Coefficient in Global Annual Precipitation Data, and Its Role in Characterising Regional Precipitation Deficits within a Naturally Changing Climate. *Hydrology*, 9(11), 199. doi: 10.3390/hydrology9110199

Papoulacos, K., Iliopoulos, T., Dimitriadis, P., Tsaknias, D., & Koutsoyiannis, D. (2025). Spatiotemporal Clustering of Streamflow Extremes and Relevance to Flood Insurance Claims: A Stochastic Investigation for the Contiguous USA. *Natural Hazards*, 121(1), 447–484. doi: 10.1007/s11069-024-06766-z

Pappalardo, V., & La Rosa, D. (2023). Spatial Analysis of Flood Exposure and Vulnerability for Planning More Equal Mitigation Actions. *Sustainability*, 15(10), 7957. doi: 10.3390/su15107957

Peiris, M. T. O. V. (2024). Assessment of Urban Resilience to Floods: A Spatial Planning Framework for Cities. *Sustainability*, 16(20), 9117. doi: 10.3390/su16209117

Pejabat Daerah dan Tanah Padang Terap. (2016). *Profail Daerah Padang Terap. Laman Rasmi*. Retrieved from <https://web.archive.org/web/20171219153106/http://ptpt.kedah.gov.my/index.php/profail-jabatan/mengenai-kami/43-perhildmatan>

Redzuan, M. S., Masron, T., Ahmad, A., Abdillah, K. K., Yusuf, A., Junaini, S. N., Jamian, M. A. H., Kimura, Y., Rainis, R., & Jubit, N. (2025). Assessing Malaysia's Urban Security through ESHA: A Spatiotemporal Investigation of Burglary Patterns within Police Jurisdictions of Selangor, Kuala Lumpur, and Putrajaya. *International Journal of Geoinformatics*, 21(3), 29–49. doi: 10.52939/ijg.v21i3.3991

Reliefweb. (2010). *Malaysia: Floods - Aug 2010*. Retrieved from <https://reliefweb.int/disaster/fl-2010-000161-mys>

Reliefweb. (2024). *Malaysia: Floods - Nov 2024*. Retrieved from <https://reliefweb.int/disaster/fl-2024-000218-mys?utm>

Reliefweb. (2025). *Malaysia Flood 2024 - DREF Operational Update (MDRMY011)*. Retrieved from <https://reliefweb.int/report/malaysia/malaysia-flood-2024-dref-operational-update-mdrmy011?utm>

Rezende, O. M., Ribeiro da Cruz de Franco, A. B., Beléño de Oliveira, A. K., Miranda, F. M., Pitzer Jacob, A. C., Martins de Sousa, M., & Miguez, M. G. (2020). Mapping the Flood Risk to Socioeconomic Recovery Capacity Through a Multicriteria Index. *Journal of Cleaner Production*, 255(120251). doi: 10.1016/j.jclepro.2020.120251

Romali, N. S., & Yusop, Z. (2021). Establishment of Flood Damage Function Model for Urban Area in Kuantan: A Preliminary Study. *IOP Conference Series: Materials Science and Engineering*, 1144(012066). doi: 10.1088/1757-899X/1144/1/012066

Rosmadi, H. S., Ahmed, M. F., Mokhtar, M. Bin, & Lim, C. K. (2023). Reviewing Challenges of Flood Risk Management in Malaysia. *Water*, 15(13), 2390. doi: 10.3390/w15132390

Rubio, C. J., Yu, I. S., Kim, H. Y., & Jeong, S. M. (2020). Index-based Flood Risk Assessment for Metro Manila. *Water Supply*, 20(3), 851–859. doi: 10.2166/ws.2020.010

Said, M. Z. (2017). *Vulnerability and Adaptation of Flood Victims in Padang Terap District, Kedah* [Unpublished PhD Thesis]. Universiti Sains Malaysia.

Said, M. Z., Abdul Gapor, S., & Hamat, Z. (2024). Flood Vulnerability and Adaptation Assessment in Padang Terap District, Kedah, Malaysia. *Planning Malaysia: Journal of the Malaysian Institute of Planners*, 22(2), 1–16. doi: 10.21837/pm.v22i31.1450

Salignac, F., Hanoteau, J., & Ramia, I. (2022). Financial Resilience: A Way Forward Towards Economic Development in Developing Countries. *Social Indicators Research*, 160(1), 1–33. doi: 10.1007/s11205-021-02793-6

Satriano, V., Ciancia, E., Pergola, N., & Tramutoli, V. (2024). A First Extension of the Robust Satellite Technique RST-FLOOD to Sentinel-2 Data for the Mapping of Flooded Areas: The Case of the Emilia Romagna (Italy) 2023 Event. *Remote Sensing*, 16(18), 3450. doi: 10.3390/rs16183450

Seifi, M., Haron, S. H., Abdullah, A., Masron, T., Nordin, M. N., Seifi, M., & Salah, T. (2020). Applying Geographic Information System to Locate the Residential Burglary Hotspots in Penang Island, Malaysia. *Test Engineering & Management*, 83, 13840–13846.

Shahrulnizam, M., Adzim, S., & Kamaruddin, S. (2020). Flood Mitigation Measures in Urban Areas of Malaysia Using the Integrated Catchment Modelling Approach. *IOP Conference Series: Earth and Environmental Science*, 479(012014). doi: 10.1088/1755-1315/479/1/012014

Shrestha, S., Dahal, D., Poudel, B., Banjara, M., & Kalra, A. (2025). Flood Susceptibility Analysis with Integrated Geographic Information System and Analytical Hierarchy Process: A Multi-Criteria Framework for Risk Assessment and Mitigation. *Water*, 17(7), 937. doi: 10.3390/w17070937

Sibandze, P., Kalumba, A. M., H. Aljaddani, A., Zhou, L., & Afuye, G. A. (2025). Geospatial Mapping and Meteorological Flood Risk Assessment: A Global Research Trend Analysis. *Environmental Management*, 75, 137–154. doi: 10.1007/s00267-024-02059-0

Singer, M. (2018). Climate Change and Social Inequality. Routledge. doi: 10.4324/9781315103358

Stock, A. (2025). Choosing Blocks for Spatial Cross-Validation: Lessons from a Marine Remote Sensing Case Study. *Frontiers in Remote Sensing*, 6(1531097). doi: 10.3389/frsen.2025.1531097

Tanoue, M., Taguchi, R., Alifu, H., & Hirabayashi, Y. (2021). Residual Flood Damage under Intensive Adaptation. *Nature Climate Change*, 11, 823–826. doi: 10.1038/s41558-021-01158-8

The Star. (2010). Floods: More Evacuated in Kedah and Perlis. The Star. Retrieved from <https://www.thestar.com.my/news/nation/2010/11/04/floods-more-evacuated-in-kedah-and-perlis?utm>

United Nations Office for Disaster Risk Reduction (UNDRR). (2025). *Vulnerability: Understanding Disaster Risk. Prevention Web*. Retrieved from <https://www.preventionweb.net/understanding-disaster-risk/component-risk/vulnerability#>

United Nations. (2023). *Flood Management and Climate Change Adaptation in Malaysia. Department of Economic and Social Affairs, Sustainable Development*. Retrieved from <https://sdgs.un.org/partnerships/flood-management-and-climate-change-adaptation-malaysia>

Utama, L., Amrizal, Berd, I., & Zuherna. (2019). Flood Debit Analysis Based on Land Use: A Case of Batang Arau Watershed, Padang. *IOP Conference Series: Earth and Environmental Science*, 343(012003), 1–5. doi: 10.1088/1755-1315/343/1/012003

Wang, N., Sun, F., Koutsoyiannis, D., Iliopoulos, T., Wang, T., Wang, H., Liu, W., Sargentis, G. -Fivos, & Dimitriadis, P. (2023). How can Changes in the Human-Flood Distance Mitigate Flood Fatalities and Displacements? *Geophysical Research Letters*, 50(20). doi: 10.1029/2023GL105064

Wang, Y., Li, H., Shi, Y., & Yao, Q. (2022). A Study on Spatial Accessibility of the Urban Stadium Emergency Response under the Flood Disaster Scenario. *Sustainability*, 14(24), 17041. doi: 10.3390/su142417041

Wing, O. E. J., Lehman, W., Bates, P. D., Sampson, C. C., Quinn, N., Smith, A. M., Neal, J. C., Porter, J. R., & Kousky, C. (2022). Inequitable Patterns of US Flood Risk in the Anthropocene. *Nature Climate Change*, 12, 156–162. doi: 10.1038/s41558-021-01265-6

Yusoff, N. A., Shafii, H., & Omar, R. (2017). The Impact of Floods in Hospital and Mitigation Measures: A Literature Review. *IOP Conference Series: Materials Science and Engineering*, 271(012026). doi: 10.1088/1757-899X/271/1/012026

Zakaria, Y. S., Ahmad, A., Said, M. Z., Epa, A. E., Ariffin, N. A., M Muslim, A., Akhir, M. F., & Hussin, R. (2023). GIS and Oil Spill Tracking Model in Forecasting Potential Oil Spill-Affected Areas Along Terengganu and Pahang Coastal Area. *Planning Malaysia: Journal of the Malaysian Institute of Planners*, 21(4), 250–264. doi: 10.21837/pm.v21i28.1330

Zakaria, Y. S., Akhir, M. F., Muslim, A. M., Ariffin, N. A., & Ahmad, A. (2025). Estimating Forest Aboveground Biomass Density Using Remote Sensing and Machine Learning: A RSME Approach. *Land Degradation & Development. Land Degradation & Development*, 36(18), 6514–6527. doi: 10.1002/lrd.70087

Zakaria, Y. S., Ariffin, N. A., Ahmad, A., Rainis, R., M. Muslim, A., & Wan Ibrahim, W. M. M. (2025). Optimizing Tuberculosis Treatment Predictions: A Comparative Study of XGBoost with Hyperparameter in Penang, Malaysia (Mengoptimalkan Peramalan Rawatan Tuberkulosis: Suatu Kajian Perbandingan XGBoost dengan Hiperparameter di Penang, Malaysia). *Sains Malaysiana*, 54(1), 3743–3754. doi: 10.17576/jsm-2025-5401-22

Zhang, H., Luo, J., Wu, J., & Yu, M. (2022). Spatial-Temporal Characteristics and Driving Factors of Flash Floods in Shaanxi Province Considering Regional Differentiation. *Hydrology Research*, 53(1), 156–174. doi: 10.2166/nh.2021.103

Zhou, C., Shen, H., Wu, H., Li, J., Wang, C., & Du, S. (2025). A Spatial-Explicit Analysis of Influencing Factors of Observed Floods in the Yangtze River Delta, China. *Landscape Ecology*, 40(180). doi: 10.1007/s10980-025-02201-1

Zhou, X., Ma, W., Echizenya, W., & Yamazaki, D. (2021). The Uncertainty of Flood Frequency Analyses in Hydrodynamic Model Simulations. *Natural Hazards and Earth System Sciences*, 21(3), 1071–1085. doi: 10.5194/nhess-21-1071-2021